

Appendices

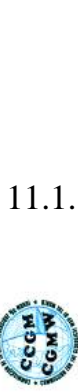
MSc Thesis
Matthijs A. Hogerwerf*
*e-mail: M.A.Hogerwerf@gmail.com

July 2010
Faculty of Geosciences
Utrecht University

Supervisor:
Dr. H.L.M. van Roermund

Table of contents

11.1.	International geological time scale chart.....	2
11.2.	Geological maps of the fieldwork area	3
11.3.	Thin sections, monazite locations and BSE images Marsfjället area.....	9
11.4	Thin sections, monazite locations and BSE images Avarado and Sjouten gneiss (HP units).....	36
11.5.	Thin sections, monazite locations and BSE images Svartsjöbäcken schist.	63
11.6.	Calculations XRF	67
11.7.	Mineral list Theriak-Domino	69
11.8.	Original tectonostratigraphic map Gee (1985).....	72
11.9.	Poster.....	73
11.10.	Overview digital MSc Thesis M.A.Hogerwerf.....	74



A Proposal for Simplifying the International Geological Time Scale Chart



Appendix 11.1: Tme table after ICS. (International Commission on Stratigraphy 2008).

Erathem	System Period	Series Epoch	Stage Age	Age Ma	GSSP	
Cenozoic	Quaternary*	Anthropocene		1800 AD		
		Holocene	Upper	0.0118		
		Pleistocene	Middle	0.126		
			Lower	0.781		
	Neogene	Pliocene	Gelasian	1.806		
			Piacenzian	2.588		
		Miocene	Zandean	3.600		
			Messinian	5.332		
			Tortonian	7.246		
	Tertiary*	Oligocene	Serravallian	11.608		
			Langhian	13.82		
		Eocene	Burdigalian	15.97		
			Aquitanian	20.43		
	Paleogene	Oligocene	Chattian	28.4 ± 0.1		
			Rupelian	33.9 ± 0.1		
			Priabonian	37.2 ± 0.1		
		Eocene	Bartonian	40.4 ± 0.2		
Lutetian			48.6 ± 0.2			
Paleocene		Ypresian	55.8 ± 0.2			
		Thanetian	58.7 ± 0.2			
Cretaceous		Upper	Selandian	61.7 ± 0.2		
			Danian	65.5 ± 0.3		
			Maestrichtian	70.6 ± 0.6		
Mesozoic	Upper	Campanian	83.5 ± 0.7			
		Santonian	85.8 ± 0.7			
		Coniacian	88.3 ± 1.0			
	Middle	Turonian	93.5 ± 0.8			
		Cenomanian	98.6 ± 0.9			
		Albian	112.0 ± 1.0			
		Aptian	125.0 ± 1.0			
	Lower	Barremian	130.0 ± 1.5			
		Hauterivian	135.4 ± 2.0			
		Valanginian	140.2 ± 3.0			
Paleozoic	Permian	Lower	Berrislian	145.5 ± 4.0		
			Wuchiapingian	253.8 ± 0.7		
			Changhsingian	259.4 ± 0.7		
		Middle	Wuchiapingian	260.4 ± 0.7		
			Capitanian	265.8 ± 0.7		
		Upper	Wordian	268.0 ± 0.7		
			Roadian	270.6 ± 0.7		
			Kungurian	275.6 ± 0.7		
		Carboniferous	Upper	Asselian	294.4 ± 0.8	
				Gzhelian	299.0 ± 0.8	
	Middle		Kasimovian	303.9 ± 0.9		
			Moscovian	306.5 ± 1.0		
			Bashkirian	311.7 ± 1.1		
	Lower		Serpukhovian	318.1 ± 1.3		
			Mississippian	326.4 ± 1.6		
	Silurian	Lower	Tournaisian	345.3 ± 2.1		
			Visean	359.2 ± 2.5		
Stenonian			419.7 ± 2.7			
Middle		Pragian	411.2 ± 2.8			
		Lochkovian	416.0 ± 2.8			
Upper		Pridoli	421.3 ± 2.6			
		Ludlow	423.9 ± 2.5			
		Gorstian	429.2 ± 2.3			
		Homerian	436.0 ± 1.9			
		Sherwoodian	439.0 ± 1.8			
Devonian	Lower	Frasnian	374.5 ± 2.6			
		Givetian	391.8 ± 2.7			
		Emsian	397.5 ± 2.7			
	Middle	Famennian	359.2 ± 2.5			
		Frasnian	365.3 ± 2.6			
	Upper	Pragian	407.0 ± 2.8			
		Emsian	412.2 ± 2.8			
		Lochkovian	416.0 ± 2.8			
		Ludlowian	419.7 ± 2.7			
		Gorstian	421.3 ± 2.6			
Cambrian	Lower	Fortunian	542.0 ± 1.0			
		Stage 2	521.0 ± 0.6			
		Stage 3	517.0 ± 0.6			
	Middle	Stage 4	510.0 ± 0.6			
		Stage 5	506.5 ± 0.6			
	Upper	Drumian	503.0 ± 0.6			
		Palbian	501.0 ± 2.0			
		Stage 7	496.0 ± 0.6			
	Ordovician	Lower	Temabocian	488.3 ± 1.7		
			Floian	473.6 ± 1.7		
Capitanian			471.8 ± 1.6			
Middle		Dumortierian	469.9 ± 1.6			
		Sandbian	455.8 ± 1.6			
Upper		Katian	443.7 ± 1.5			
		Hirnantian	445.6 ± 1.5			
Precambrian	Neoproterozoic	Rhuddanian	439.0 ± 1.8			
		Aeronian	436.0 ± 1.9			
		Telychian	429.2 ± 2.3			
		Sherwoodian	423.9 ± 2.5			
		Homerian	421.3 ± 2.6			
	Mesoproterozoic	Statherian	1800			
		Crosirian	2050			
		Rhyacian	2300			
	Paleoproterozoic	Siderian	2500			
		Statherian	1800			
Archean	Neoproterozoic	Statherian	1800			
		Crosirian	2050			
		Rhyacian	2300			
	Mesoproterozoic	Siderian	2500			
		Statherian	1800			
Paleoproterozoic	Siderian	2500				
	Statherian	1800				
Proterozoic	Neoproterozoic	Siderian	2500			
		Statherian	1800			
		Crosirian	2050			
		Rhyacian	2300			
		Statherian	1800			
	Mesoproterozoic	Siderian	2500			
		Statherian	1800			
		Crosirian	2050			
		Rhyacian	2300			
		Statherian	1800			
Paleoproterozoic	Siderian	2500				
	Statherian	1800				
	Crosirian	2050				
	Rhyacian	2300				
	Statherian	1800				
Eozoic	Neoproterozoic	Siderian	2500			
		Statherian	1800			
		Crosirian	2050			
		Rhyacian	2300			
		Statherian	1800			
	Mesoproterozoic	Siderian	2500			
		Statherian	1800			
		Crosirian	2050			
		Rhyacian	2300			
		Statherian	1800			
Paleoproterozoic	Siderian	2500				
	Statherian	1800				
	Crosirian	2050				
	Rhyacian	2300				
	Statherian	1800				

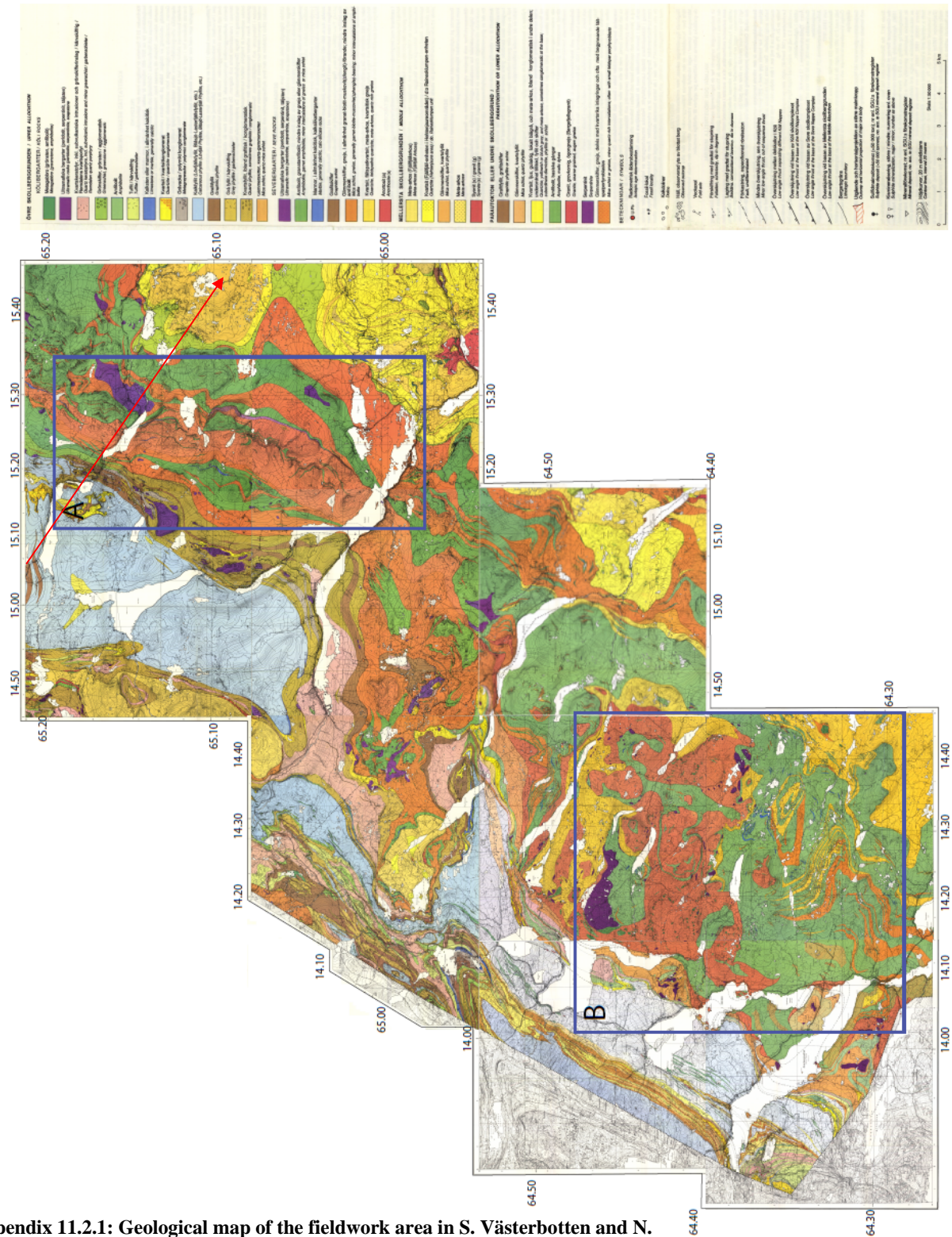
This version of the International Stratigraphic Chart contains a list of the names of the geological time scale units, including the names of the geological time scale units, rank, names and formal status are approved by the International Commission on Stratigraphy (ICS) and ratified by the International Union of Geological Sciences (IUGS). These are displayed on the regular International Stratigraphic Chart, which is available at www.stratigraphy.org. Subdivisions of the geological time scale units (where applicable) are defined by their lower boundary. Each unit of the Phanerozoic (~542 Ma to Present) and the base of Eozoic are defined by a base Global Standard Section and Point (GSSSP) whereas Precambrian units are formally subdivided by absolute age (Global Standard Stratigraphic Age, GSSA). Details of each GSSP are posted on the ICS website (www.stratigraphy.org). The listed numerical ages are from 'A Geologic Time Scale 2004' by F.M. Gradstein, J.G. Ogg, A.G. Smith, et al. (2004, Cambridge University Press). Ages of the unit boundaries in the Precambrian and Phanerozoic are subject to revision.

This chart was drafted by Gail Ogg, Intra Cambrian unit ages with * are informal and awaiting ratified definitions.

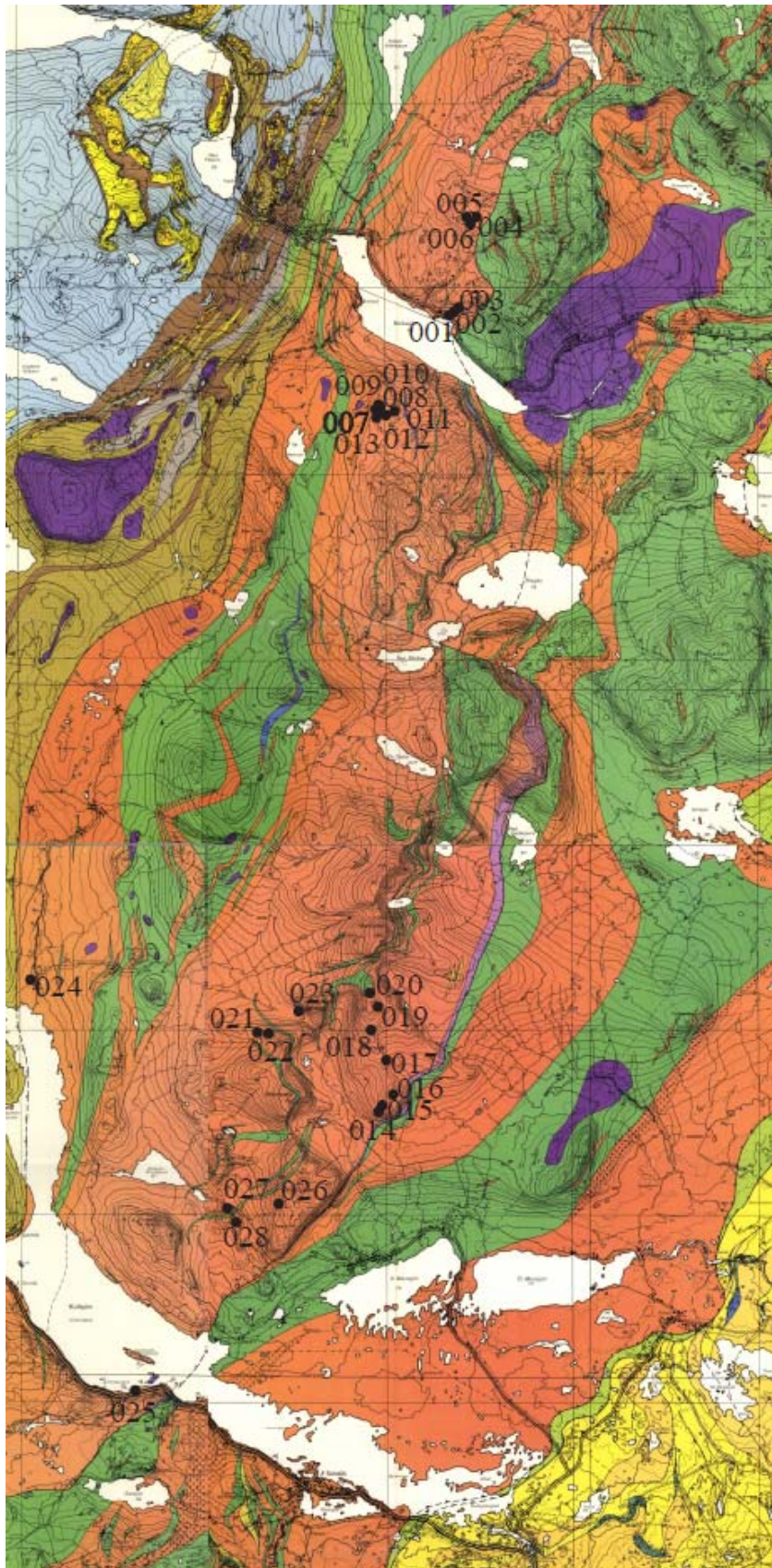
Copyright © 2007 International Commission on Stratigraphy

* Anthropocene is a chronostratigraphic unit proposed in 2007 by the Stratigraphic Commission of the Geological Society, UK. The status of the Quaternary is not yet decided. Its base may be assigned as the base of the Gelasian and extend the base of the Pleistocene to 2.6 Ma. Berris is an informal chronostratigraphic unit. (Amal, Alary et al. (2005, Episodes 28:2).

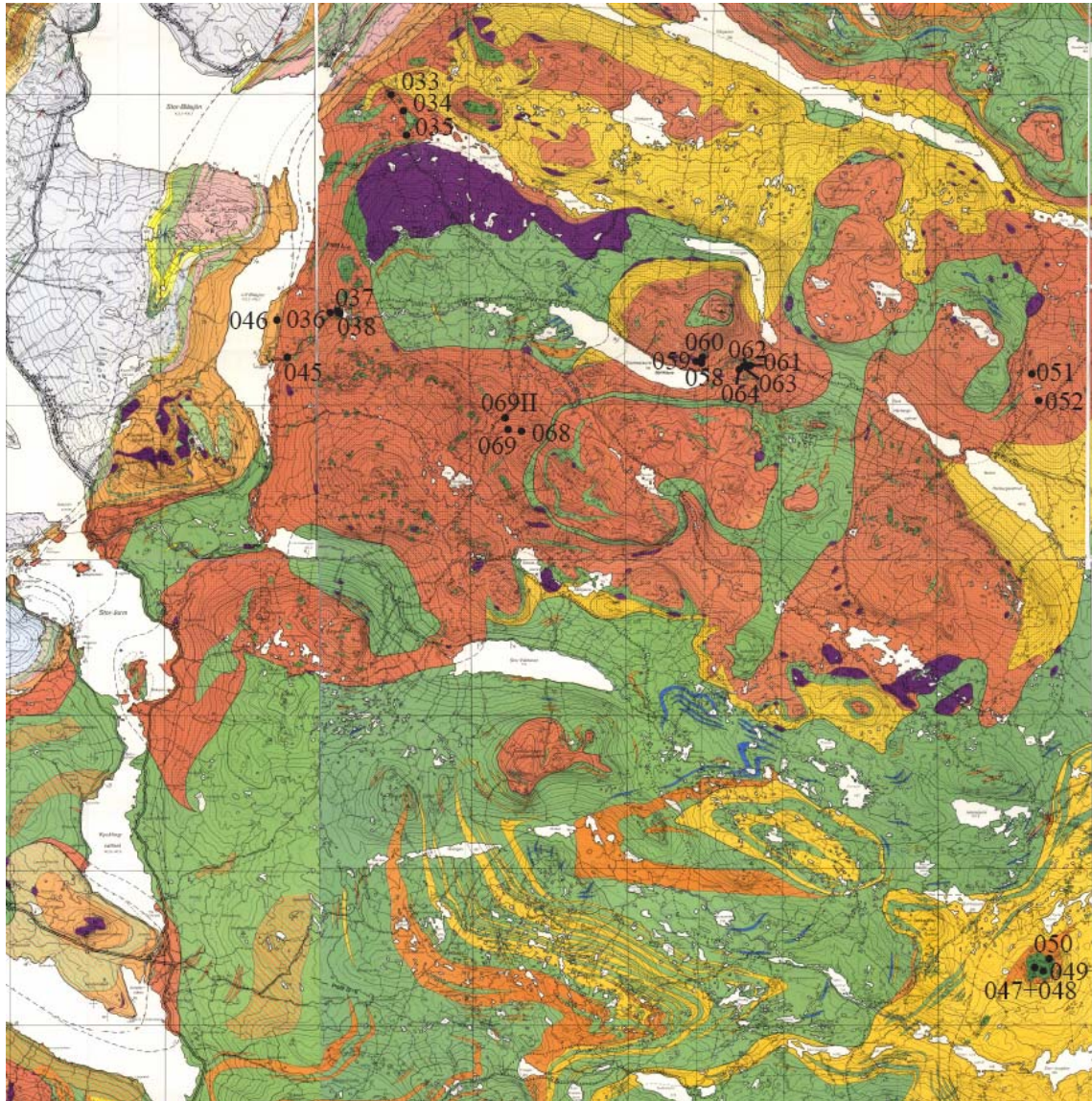
11.2. Geological maps of the fieldwork area



Appendix 11.2.1: Geological map of the fieldwork area in S. Västerbotten and N. Jämtland. Square A is contouring the Marsfjällen area. Square B is contouring the HP area. The red arrow indicates trace cross section AB. Enlargements of square A and B can be found in appendix 11.2.2 and 11.2.3. The Legend is illustrated in appendix 11.2.4. Modified after SGU 1991. Scale = 5² km² per square.



Appendix 11.2.2. Enlargement of square A, Marsfjällen area, with sample locations. Scale: Approximately 20 by 45 km (5² km² per square).










Appendix 11.2.3. Enlargement of square B, Avardo and Sjouten units, with sample locations. Scale ~ 35 by 35 km (5² km² per square).

ÖVRE SKOLLBERGGRUNDEN / UPPER ALLOCHTHON

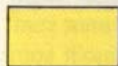
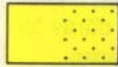

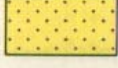

KÖLIBERGARTER / KÖLI ROCKS

	Metagabbro (grönsten, amfibolit) <i>Metagabbro (greenstone, amphibolite)</i>
	Ultramafiska bergarter (peridotit, serpentinit, täljsten) <i>Ultramafic rocks (peridotite, serpentinite, soapstone)</i>
	Kvartskeratofyr, inkl. subvulkaniska intrusioner och grönskifferinslag / kärvskiffrig / Remdalens kvartsporfy <i>Quartz keratophyre, incl. subvolcanic intrusions and minor greenschist / garbenschiefer / Remdalen quartz porphyry</i>
	Grönskiffer, grönsten / agglomeratisk <i>Greenschist, greenstone / agglomeratic</i>
	Amfibolit <i>Amphibolite</i>
	Tuffit / kärvskiffrig <i>Tuffite / garbenschiefer</i>
	Kalksten eller marmor, i allmänhet kalcitisk <i>Limestone or marble, generally calcitic</i>
	Kvartsit / kvartsitkonglomerat <i>Quartzite / quartzite conglomerate</i>
	Gråvacka / polymikt konglomerat <i>Metagreywacke / polymict conglomerate</i>
	Kalkfyllit (Lövfjällsfyllit, Blåsjö-Lasterfjällsfyllit, etc.) <i>Calcareous phyllite (Lövfjäll Phyllite, Blåsjö-Lasterfjäll Phyllite, etc.)</i>
	Grafitfyllit <i>Graphitic phyllite</i>
	Grå fyllit / kärvskiffrig <i>Grey phyllite / garbenschiefer</i>
	Kvartsfyllit, ibland grafitisk / konglomeratisk <i>Quartz phyllite, sometimes graphitic / conglomeratic</i>
	Glimmerskiffer, kvarts-glimmerskiffer <i>Mica schist, quartz-mica schist</i>

SEVEBERGARTER / SEVE ROCKS


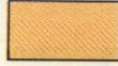
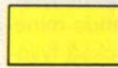




-  Ultramafiska bergarter (peridotit, serpentinit, täljsten)
Ultramafic rocks (peridotite, serpentinite, soapstone)
-  Amphibolit, granatamfibolit; mindre inslag av gnejs eller glimmerskiffer
Amphibolite, garnet amphibolite; minor intercalations of gneiss or mica schist
-  Marmor, i allmänhet kalcitisk, kalksilikatbergarter
Marble, generally calcitic, calc-silicate rocks
-  Grafitskiffer
Graphitic schist
-  Glimmerskiffer, gnejs, i allmänhet granat-biotit-muskovit(±fengit)-förande; mindre inslag av amfibolit
Mica schist, gneiss, generally garnet-biotite-muscovite(±phengite)-bearing; minor intercalations of amphibolite
-  Kvartsit, fältspatkvartsit, meta-arkos, kvartsitisk gnejs
Quartzite, feldspathic quartzite, meta-arkose, quartz-rich gneiss
-  Anortosit (a)
Anorthosite (a)

MELLERSTA SKOLLBERGGRUNDEN / MIDDLE ALLOCHTHON



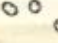
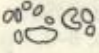
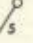
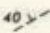
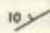
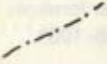

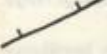
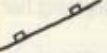

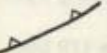



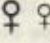


-  Meta-arkos (Fjällfjällarkos)
Meta-arkose (Fjällfjäll Arkose)
-  Kvartsit (Fjällfjäll-enheten i Hehtenjaureområdet) / d:o Rainesklumpen-enheten
Quartzite (Hehtenjaure area) / do. Rainesklumpen unit
-  Glimmerskiffer, kvartsfyllit
Mica schist, quartz phyllite
-  Meta-arkos
Meta-arkose
-  Syenit (s) / granit (g)
Syenite (s) / granite (g)

PARAUTOKTON ELLER UNDER SKOLLBERGGRUND /

PARAUTOCHTHON OR LOWER ALLOCHTHON

-  Grafitfyllit, grafitskiffer
Graphitic phyllite or schist
-  Glimmerskiffer, kvartsfyllit
Mica schist, quartz phyllite
-  Kvartsit, ljus, gulaktig, lokalt blågrå, och meta-arkos, ibland konglomeratisk i undre delen; underordnat tillitoid, fyllit och skiffer
Quartzite, yellowish or bluish grey, and meta-arkose, sometimes conglomeratic at the base; subordinate diamicite, phyllite or schist
-  Amphibolit, basiska gångar
Amphibolite, mafic dykes
-  Granit, grovkornig, ögongnejs (Bergefjellsgranit)
Granite, coarse-grained, augen gneiss
-  Serpentinit
Serpentinite
-  Glimmerskiffer, gnejs, delvis med kvartsrika inlagringar och ofta med begynnande fältspatporfyroblastes
Mica schist or gneiss, minor quartz-rich intercalations; often with small feldspar porphyroblasts

BETECKNINGAR / SYMBOLS

	Radiometrisk åldersbestämning <i>Isotopic age determination</i>
	Fossil-lokal <i>Fossil locality</i>
	Kalkböliner <i>Doline</i>
	Häll, observerad yta av blottat berg <i>Observed outcrop</i>
	Veckaxel <i>Fold axis</i>
	Förskifning med gradtal för stupning <i>Foliation, schistosity, dip in degrees</i>
	Lagring med gradtal för stupning <i>Bedding, compositional layering, dip in degrees</i>
	Förkastning, ospecificerad rörelsezon <i>Fault, undifferentiated</i>
	Mindre överskjutning, sen överskjutning <i>Minor low-angle thrust, out-of-sequence thrust</i>
	Överskjutning mellan delskollor i Köli <i>Low-angle thrust separating different Köli Nappes</i>
	Överskjutning vid basen av Köli skollkomplexet <i>Low-angle thrust at the base of the Köli Nappe Complex</i>
	Överskjutning vid basen av Seve skollkomplexet <i>Low-angle thrust at the base of the Seve Nappe Complex</i>
	Överskjutning vid basen av Mellersta skollberggrunden <i>Low-angle thrust at the base of the Middle Allochthon</i>
	Bergartsgräns <i>Lithologic boundary</i>
	Utgående och horisontalprojektion av större malmkropp <i>Outcrop and horizontal projection of major ore body</i>
	Sulfidmalmsförekomst (>50 000 ton); nr enl. SGU:s förekomstregister <i>Sulphide deposit (>50 000 tonnes); no. acc. to SGU mineral deposit register</i>
	Kismineralisering, större / mindre; numrering enl. ovan <i>Sulphide mineralization, major / minor; number as above</i>
	Mineralförekomst; nr enl. SGU:s förekomstregister <i>Mineral deposit; no. acc. to SGU mineral deposit register</i>
	Höjdkurvor, 20 m ekvidistans <i>Contour lines, interval 20 metres</i>

Skala 1:50 000

Appendix 11.2.4. Legend part 3 of 3

11.3. Thin sections, monazite locations and BSE images Marsfjället area.

In this part of the appendix, all used thin sections are illustrated with their (if present) locations of the dated monazites, BSE images of the monazite (before or after dating), locations of linescans or point measurements and BSE images of the microstructure around the dated monazite.

Samples 001-027 (*not* 024) belong to the Marsfjället gneiss. The numbers of the thin sections corresponds to the locations shown in fig. 6 and appendix 11.2.2. Some numbering issues are listed below:

- **'09Z'**-number is because these samples are taken in 2009 in Zweden. Most of the time 09Z will not be mentioned.
- Number-**'number'** corresponds to sample number-**'monazite number'**. For example: 002-6 = monazite 6 of sample 2.
- Number-number**'m'** corresponds to that particular microstructure of that monazite. For example: 004a-2m = microstructure of monazite 2 of sample 4a.
- **'L'**number = 1-number corresponds to **'number linescan'** = one to number. For example: L1=1-17 corresponds to Linescan 1 with spot analysis 1 to 17. The linescan started at the red dot in the first spot analyse.
- **'P'**number = number-number corresponds to **'point measurement number'**.

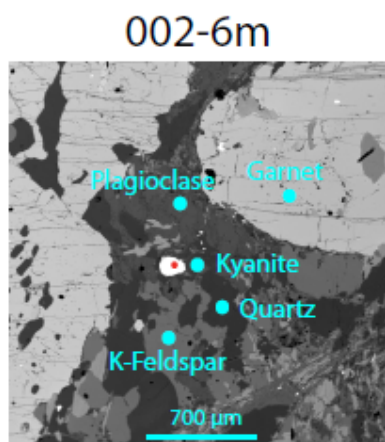
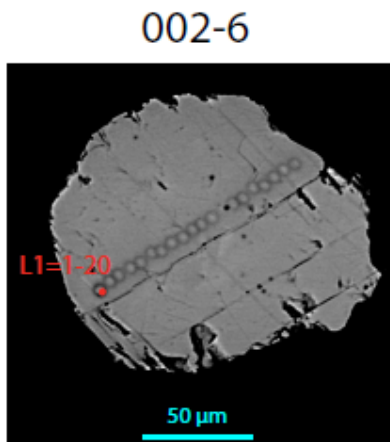
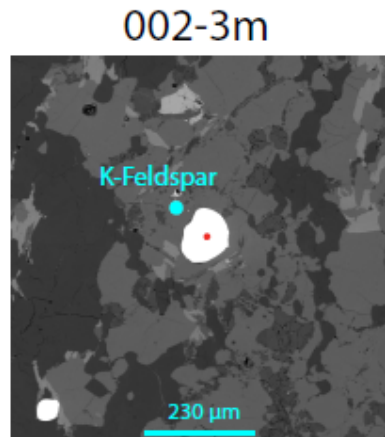
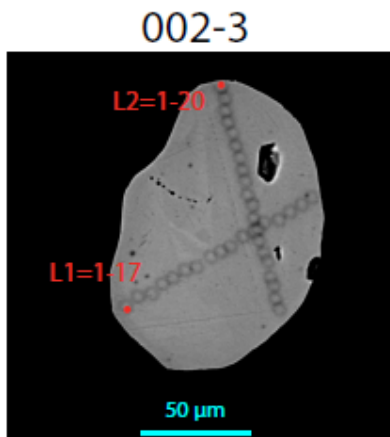
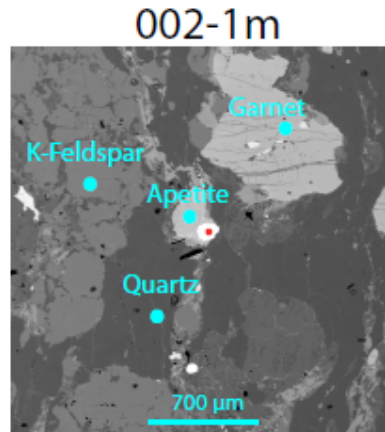
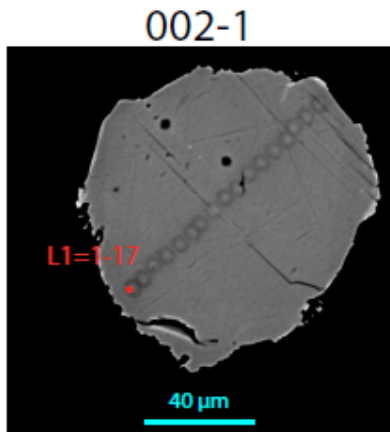
The same numbering method is used in the excel files added. So that each individual age can be traced.



Appendix 11.3. 1: Thin section of sample 09Z-001. No monazites have been dated in this sample.



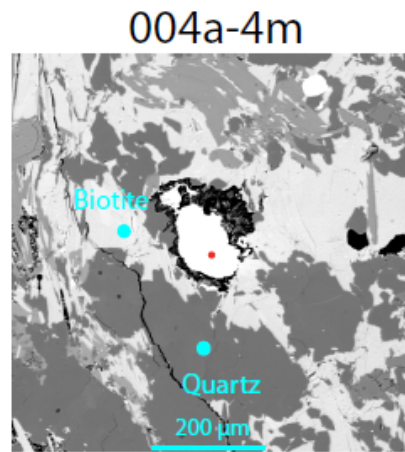
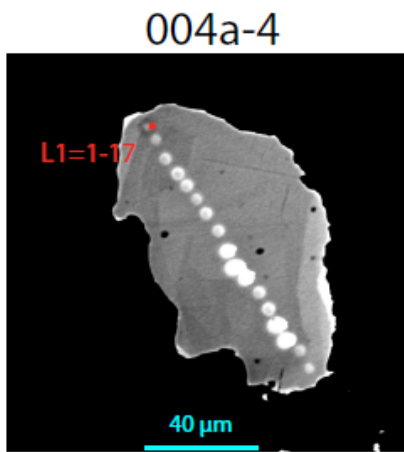
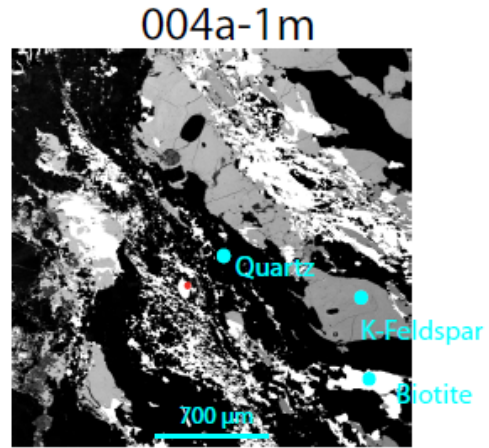
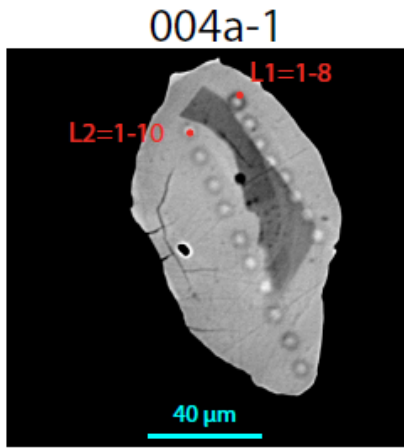
Appendix 11.3. 2: Thin section 09Z-002. Three monazites have been dated of this sample.



Appendix 11.3. 3: BSE images of dated monazites with their microstructure.



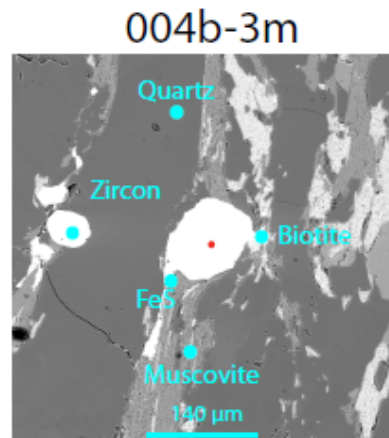
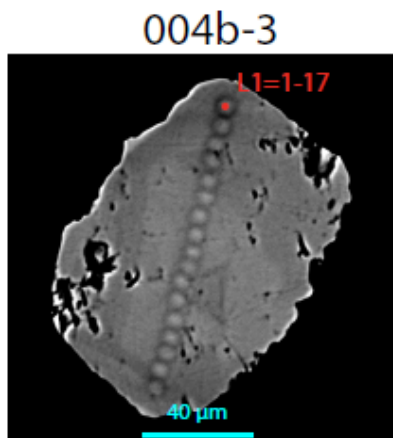
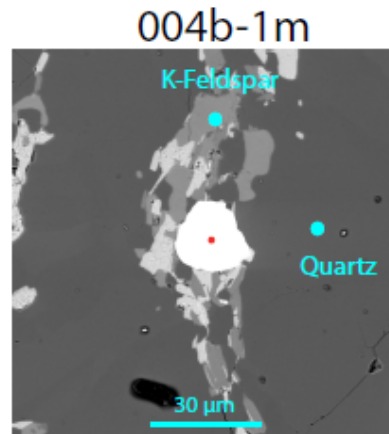
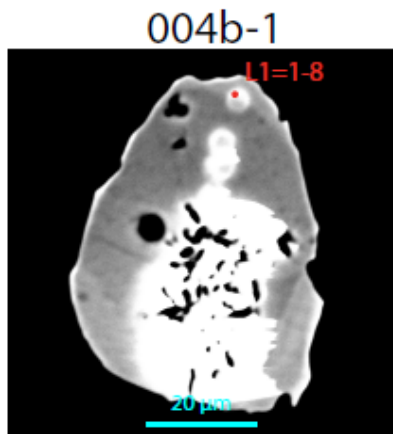
Appendix 11.3. 4: Thin section 09Z-004a. Two monazites have been dated of this sample.



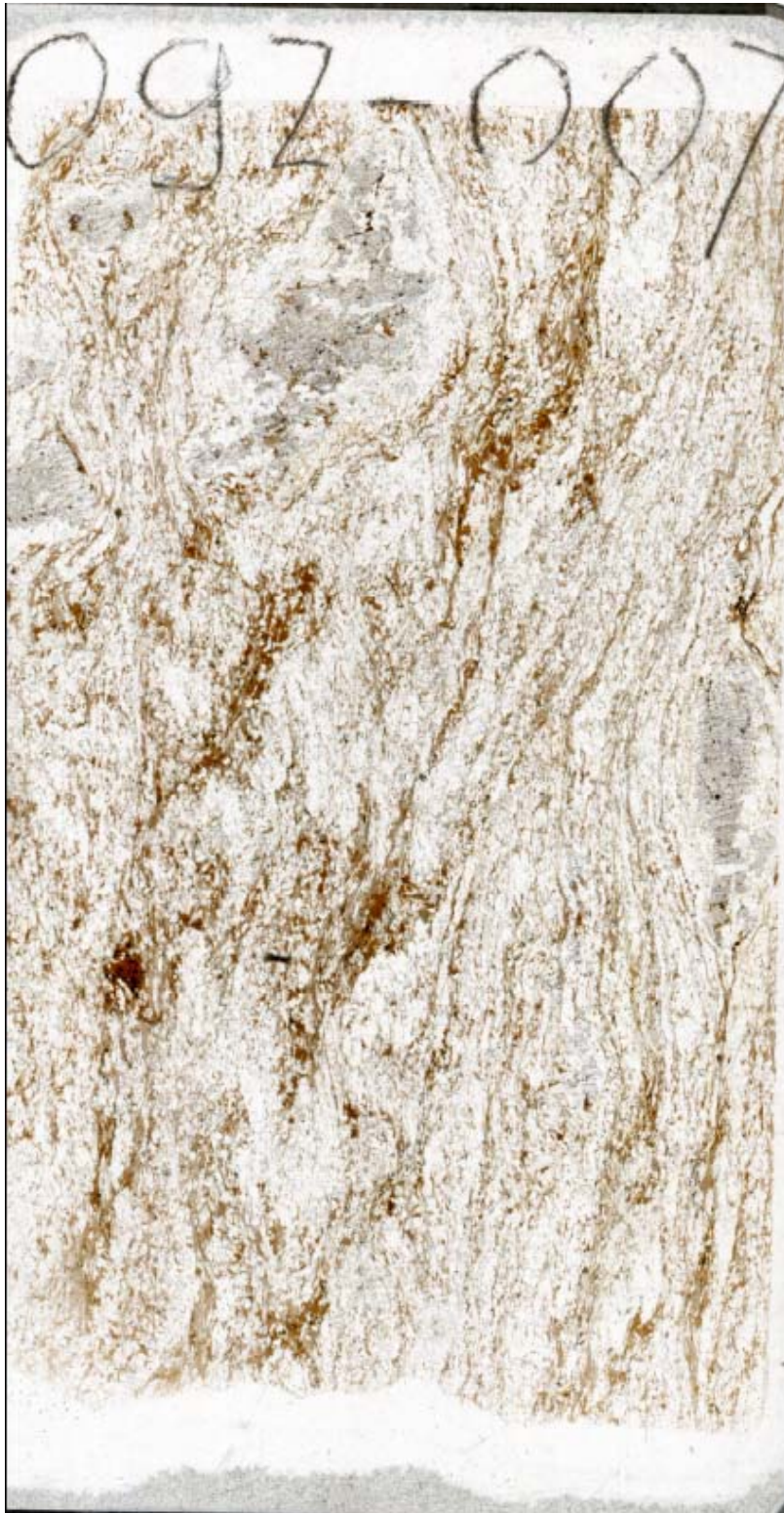
Appendix 11.3. 5: BSE images of dated monazites with their microstructure.



Appendix 11.3. 6: Thin section 09Z-004b. Two monazites have been dated of this sample.



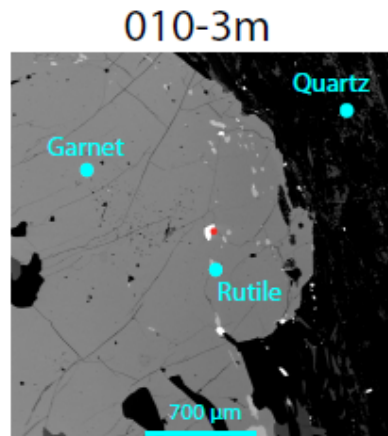
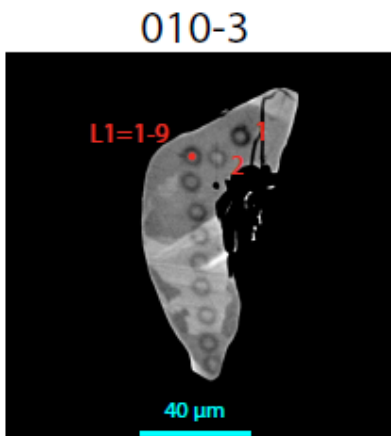
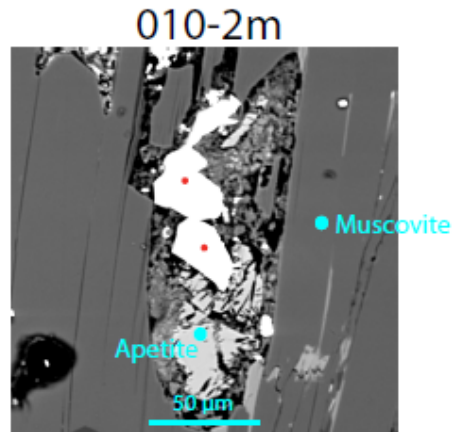
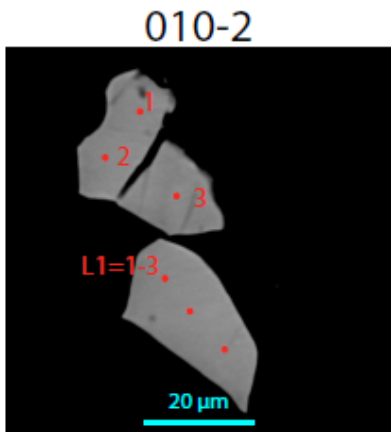
Appendix 11.3. 7: BSE images of dated monazites with their microstructure.



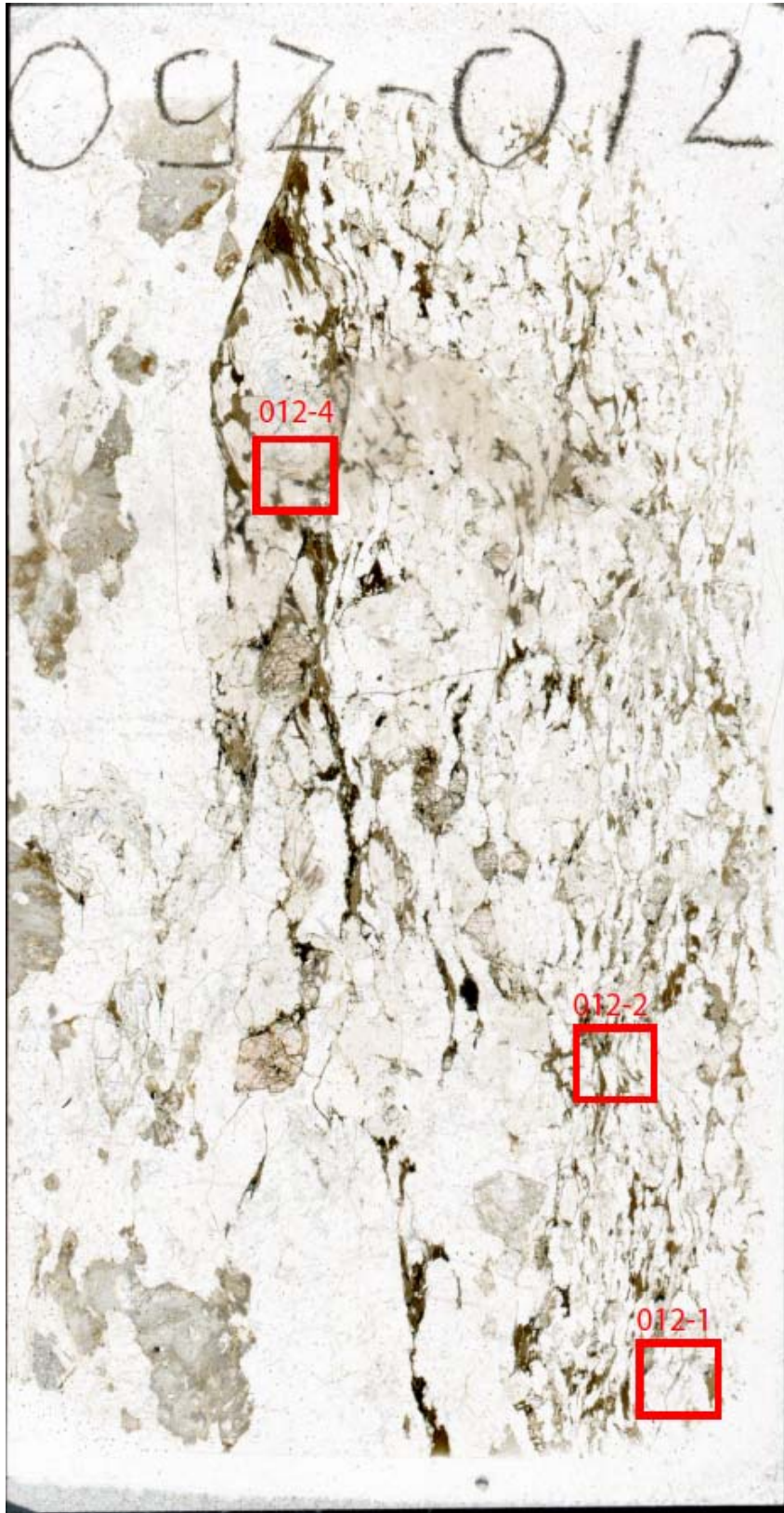
Appendix 11.3. 8: Thin section of sample 09Z-007. No monazites have been dated in this sample.



Appendix 11.3. 9: Thin section 09Z-010. Two monazites have been dated of this sample.

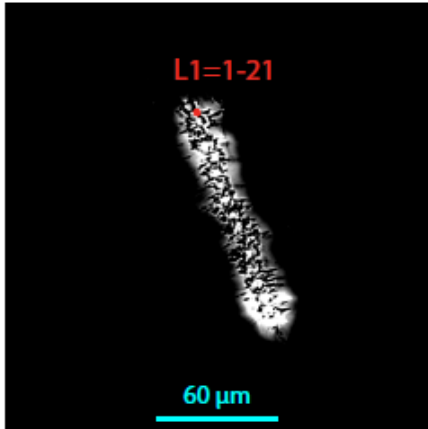


Appendix 11.3. 10: BSE images of dated monazites with their microstructure.

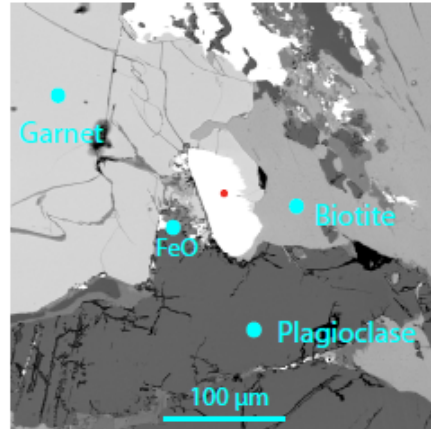


Appendix 11.3. 11: This section 09Z-012. Three monazites have been dated of this sample.

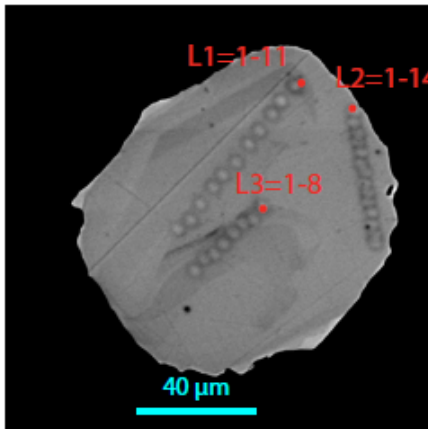
012-1



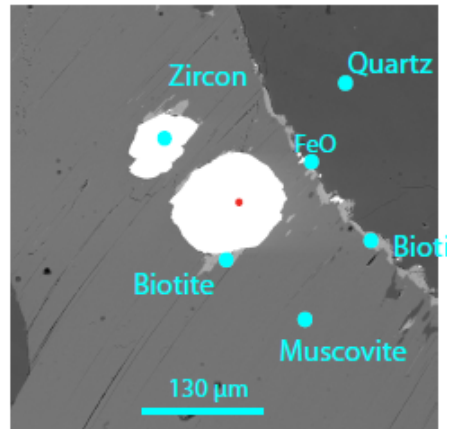
012-1m



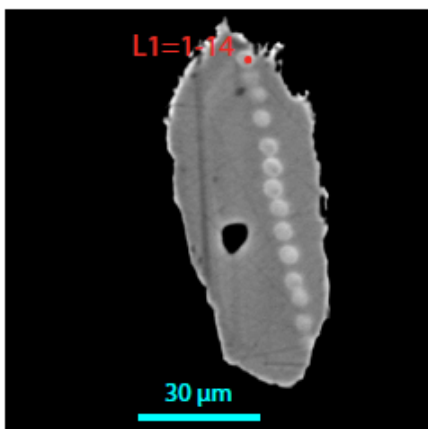
012-2



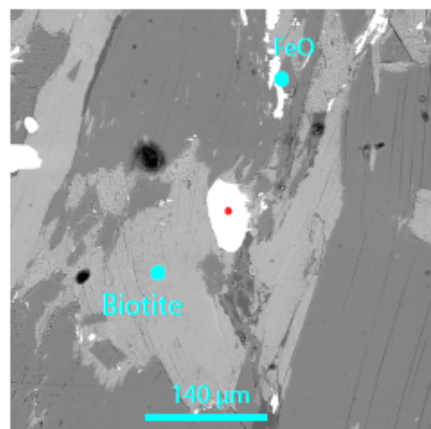
012-2m



012-4



012-4m



Appendix 11.3. 12: BSE images of dated monazites with their microstructure.

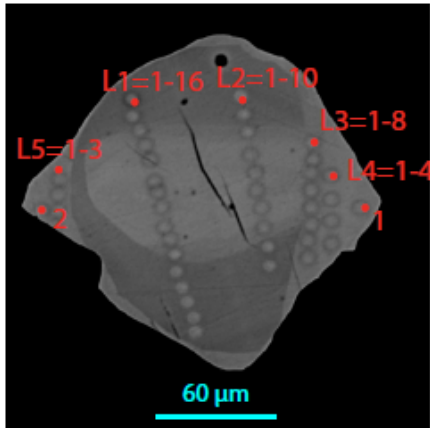


Appendix 11.3. 13: Thin section of sample 09Z-013. No monazites have been dated in this sample.

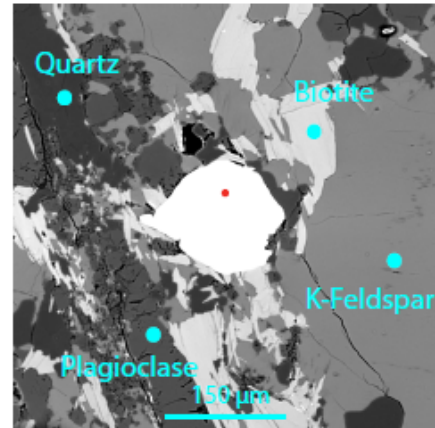


Appendix 11.3. 14: Thin section 09Z-015. Two monazites have been dated of this sample.

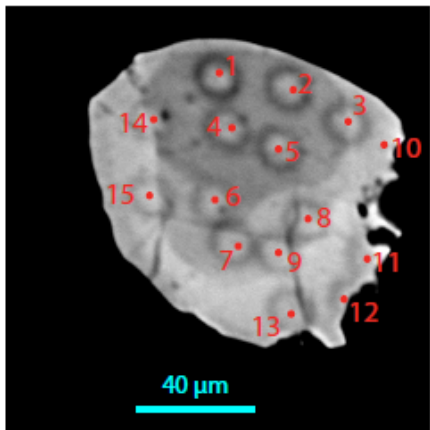
015-2



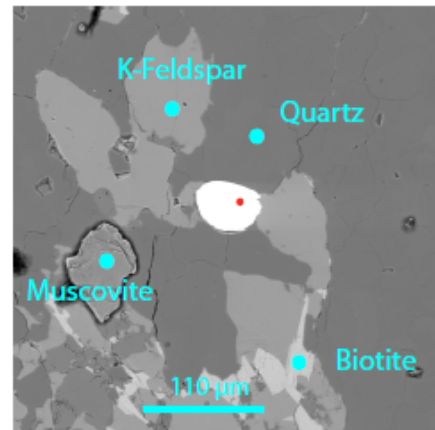
015-2m



015-3



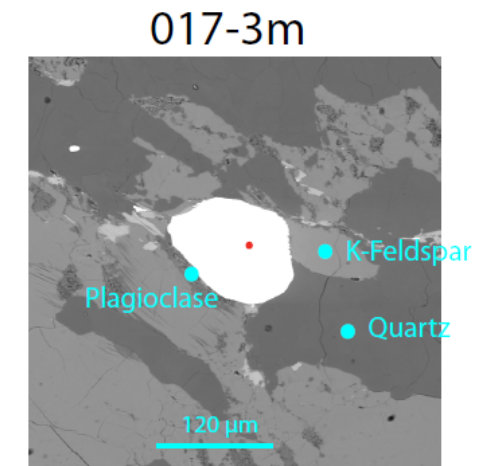
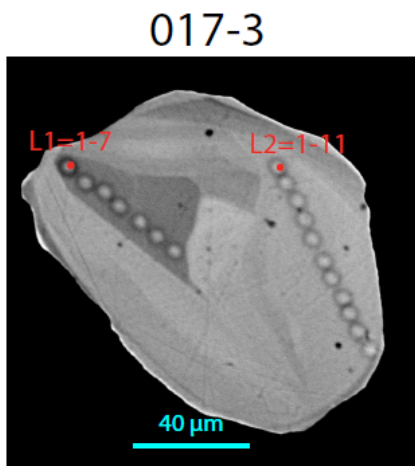
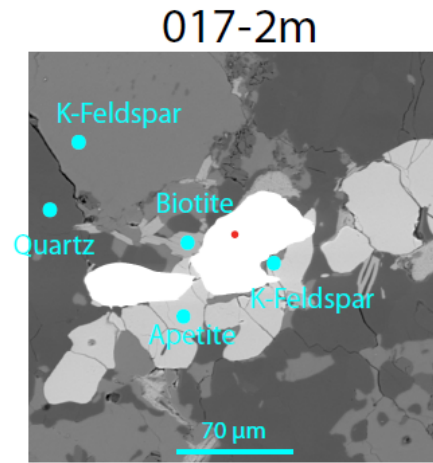
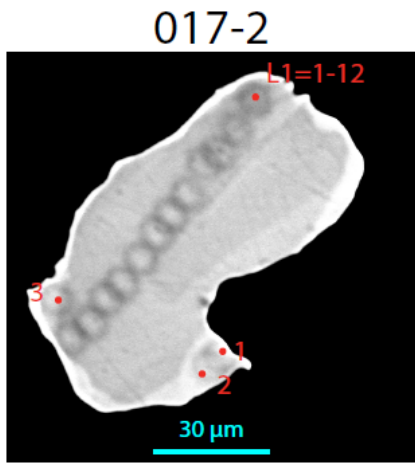
015-3m



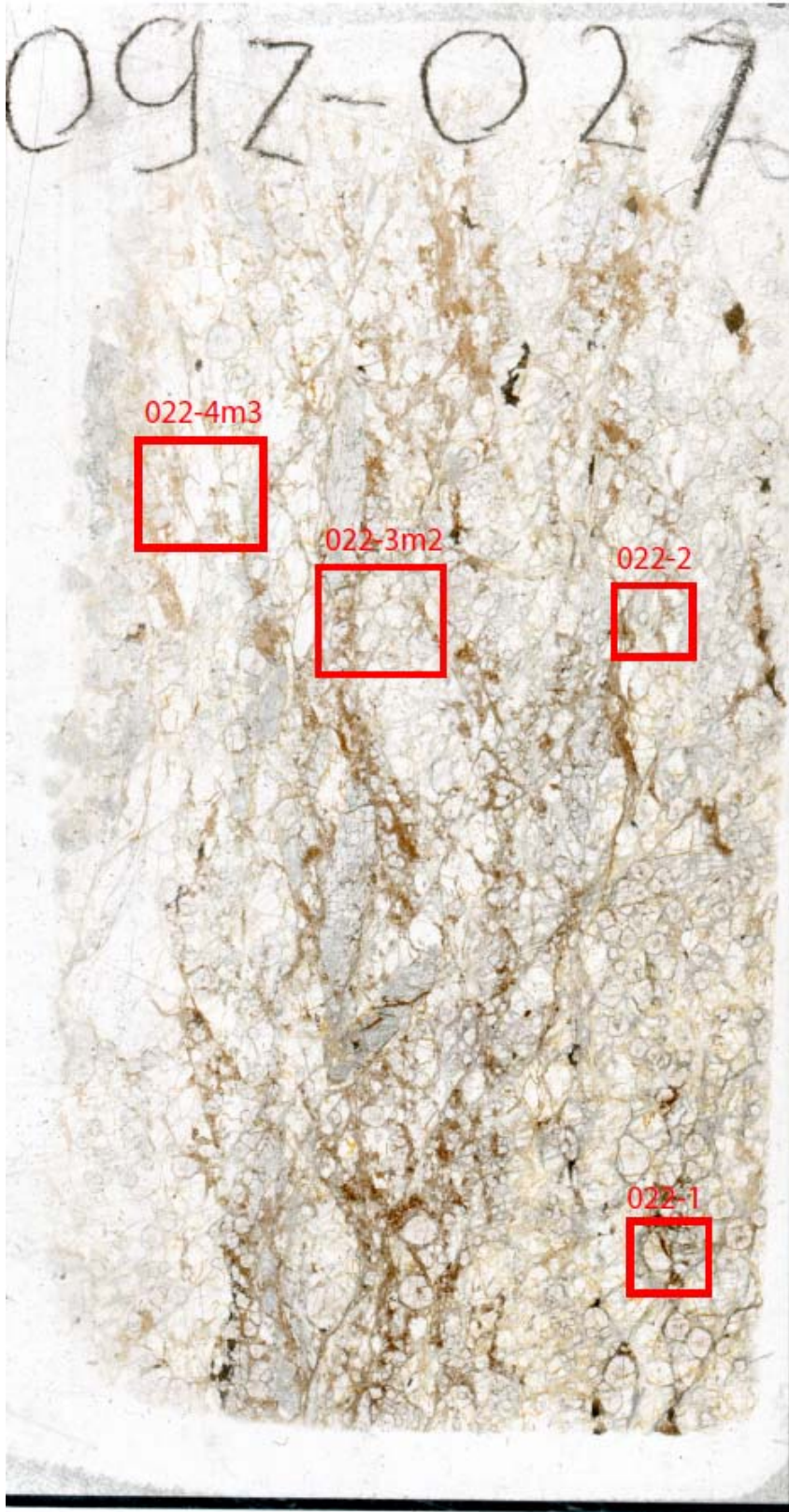
Appendix 11.3. 15: BSE images of dated monazites with their microstructure.



Appendix 11.3. 16: Thin section of sample 09Z-017. Two monazites have been measured of this sample.

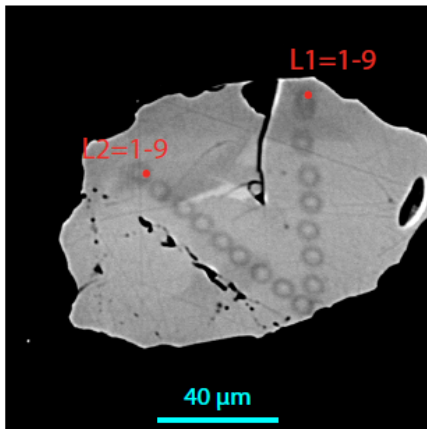


Appendix 11.3. 17: BSE images of dated monazites with their microstructure.

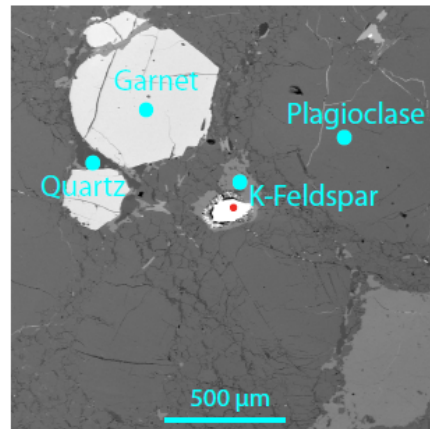


Appendix 11.3. 18: Thin section 09Z-022. Two samples have been measured of this sample.

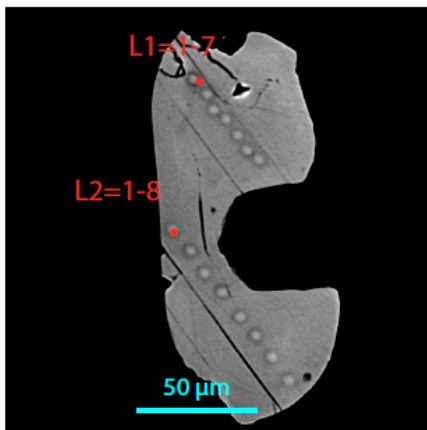
022-1



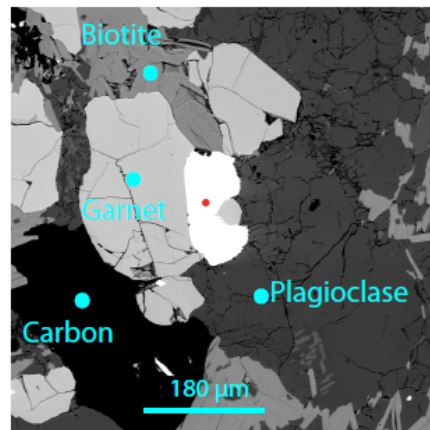
022-1m



022-2



022-2m

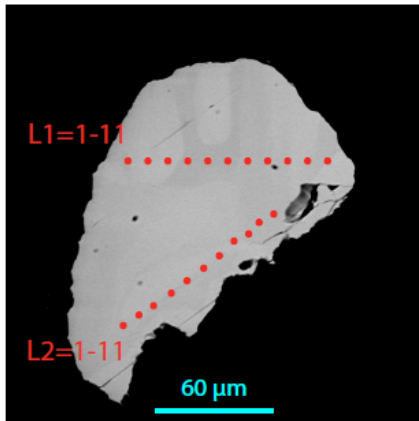


Appendix 11.3. 19: BSE images of dated monazites with their microstructure.

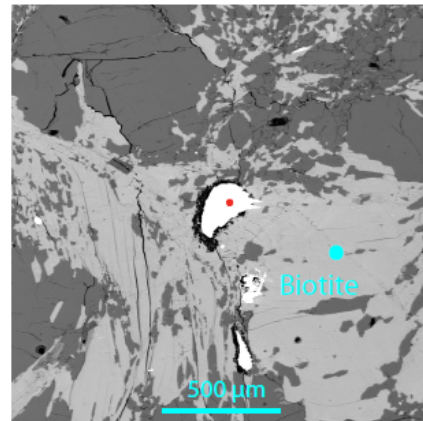


Appendix 11.3. 20: Thin section 09Z-023. Two monazites have been measured of this sample.

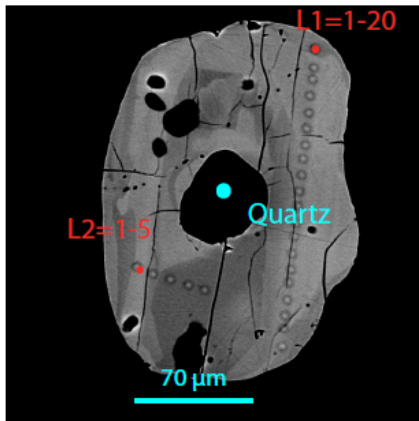
023-2



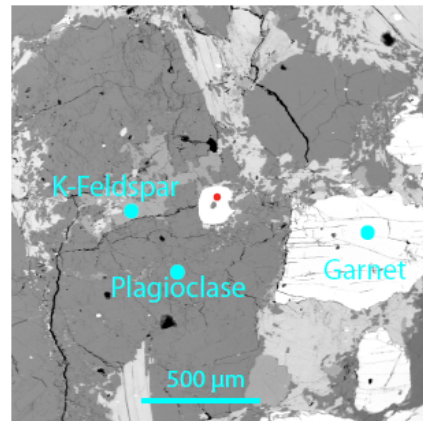
023-2m



023-4



023-4m



Appendix 11.3. 21 BSE images of dated monazites with their microstructure.

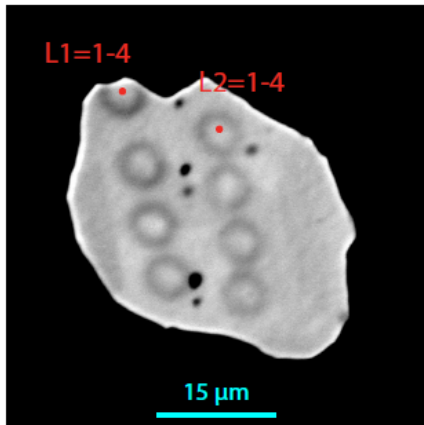


Appendix 11.3. 22: Thin section of 09Z-025. No monazites have been dated on this sample.

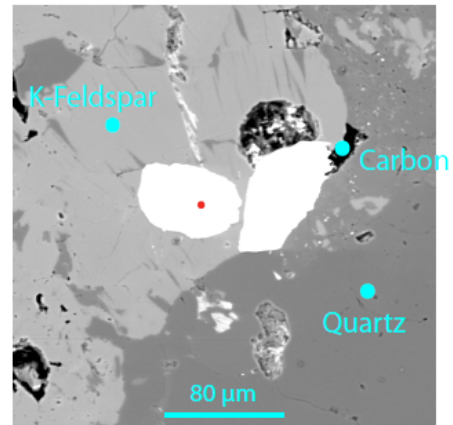


Appendix 11.3. 23: Thin section 09Z-026. Two monazites have been measured of this sample.

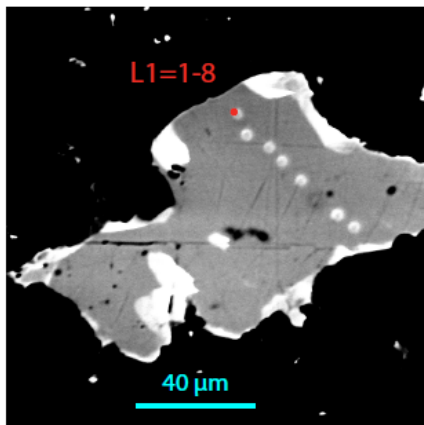
026-1



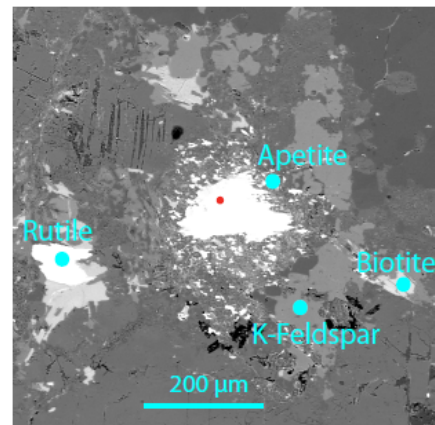
026-1m



026-3



026-3m

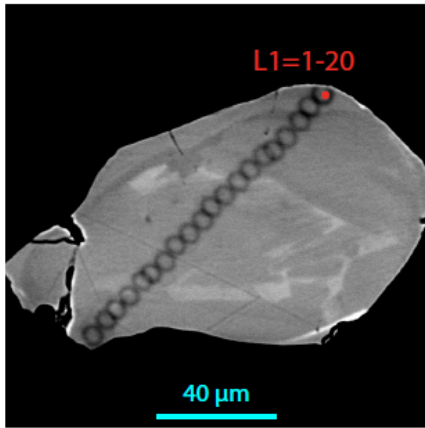


Appendix 11.3. 24: BSE images of dated monazites with their microstructure.

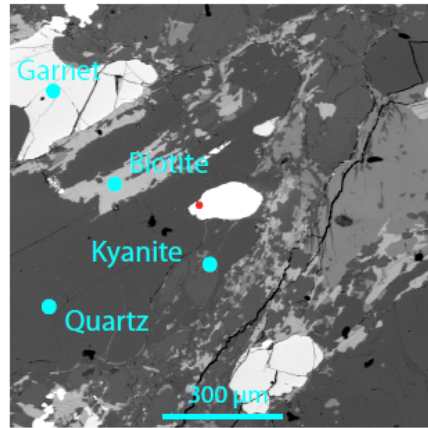


Appendix 11.3. 25: This section 09Z-027. Two monazites have been measured of this sample.

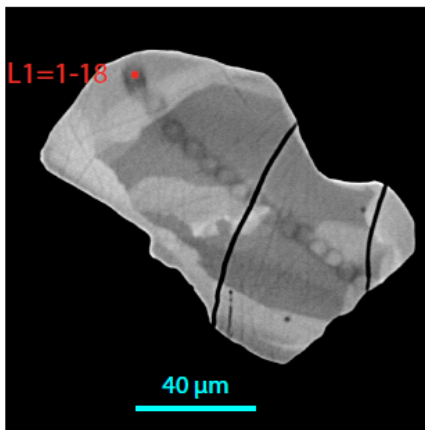
027-1



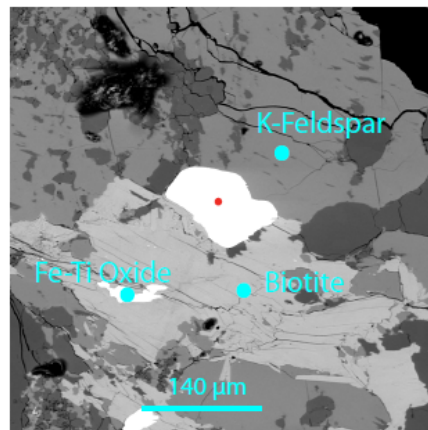
027-1m



027-3



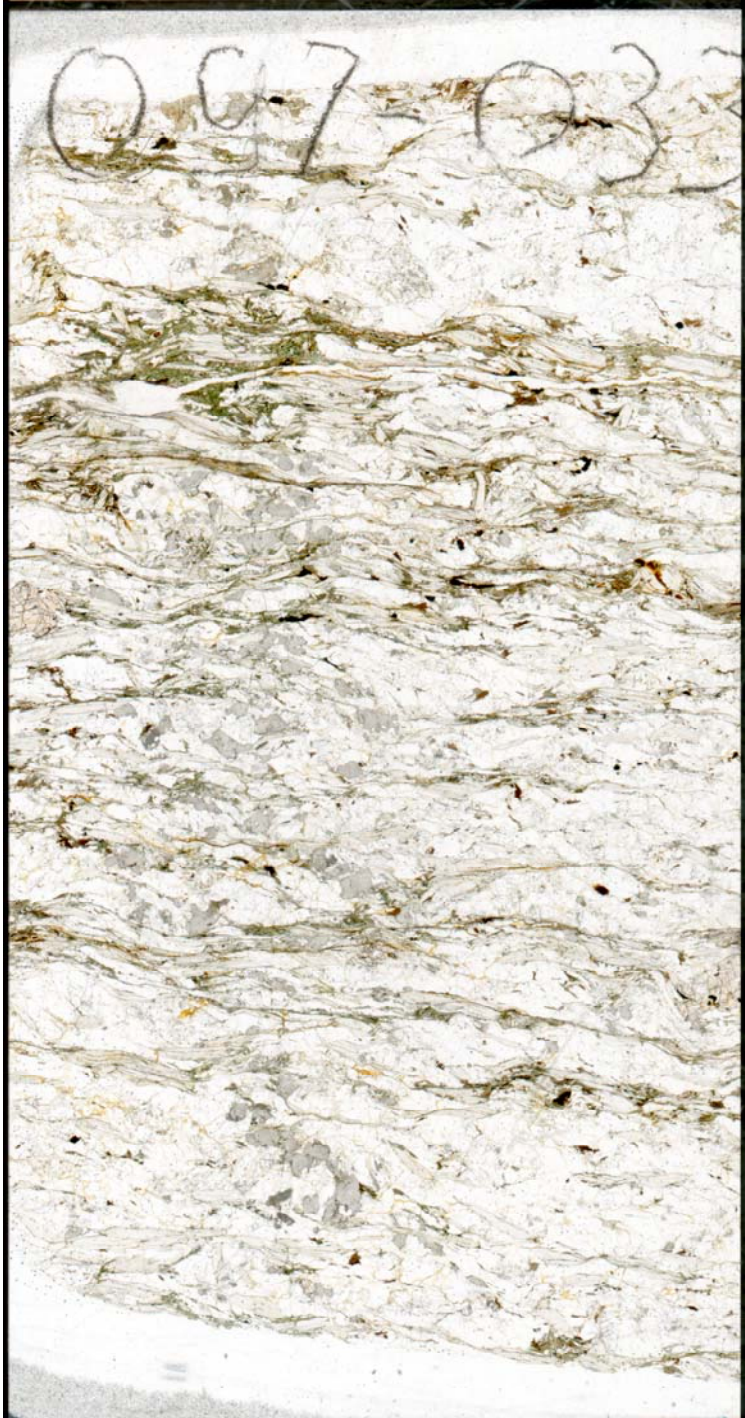
027-3m



Appendix 11.3. 26: BSE images of dated monazites with their microstructure.

11.4 Thin sections, monazite locations and BSE images Avarado and Sjouten gneiss (HP units).

Samples 33-38, 45-46, 51-52, 58-64 and 68-69II belong to the Avarado gneiss. Samples 47-50 belong to the Sjouten unit. The numbers of the thin sections corresponds to the locations shown in appendix 11.2.3.



Appendix 11.4. 1: Thin section 09Z-033. No monazites have been detected in this sample.



Appendix 11.4. 2: Thin section 09Z-034. No monazites have been dated in this sample.



Appendix 11.4. 3: Thin section 09Z-037b. No monazites have been dated in this sample.

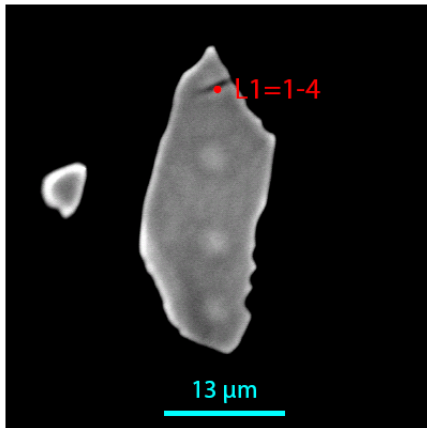


Appendix 11.4. 4: Thin section 09Z-037c. No monazites have been dated in this sample.

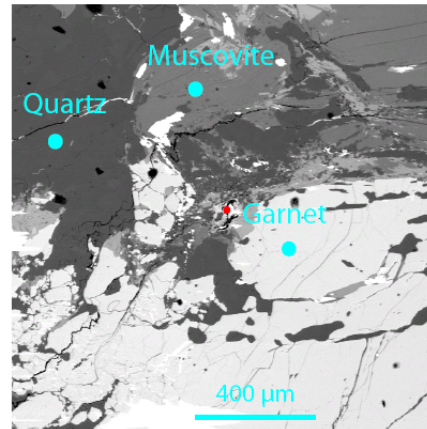


Appendix 11.4. 5: Thin section 09Z-037d. One monazite have been dated in this sample.

037d-1



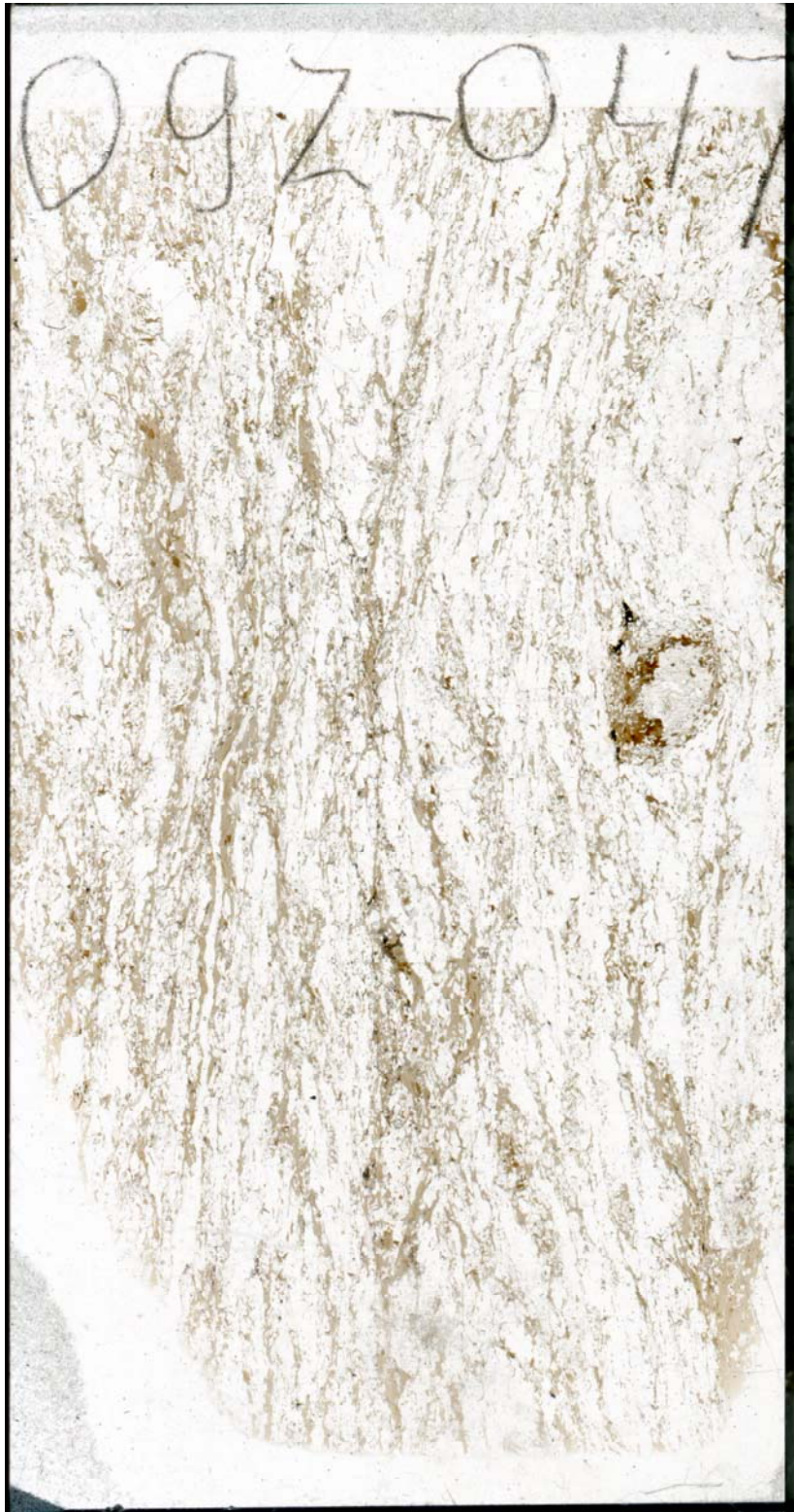
037d-1m



Appendix 11.4. 6: BSE image of dated monazite with its microstructure.



Appendix 11.4. 7: Thin section 09Z-038. No monazites have been dated in this sample.



Appendix 11.4. 8: Thin section 09Z-047. No monazites have been found in this sample.



Appendix 11.4. 9: Thin section 09Z-048. No monazites have been found in this sample.



Appendix 11.4. 10: Thin section 09Z-049b. No monazites have been found in this sample.

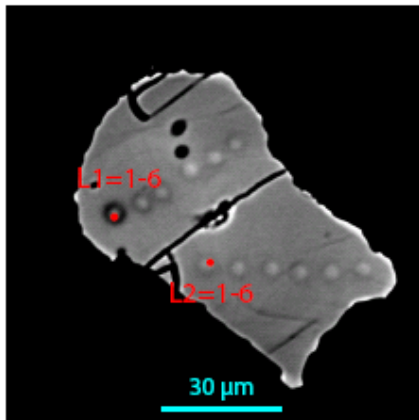


Appendix 11.4. 11: Thin section 09Z-050. No monazites have been found in this sample.

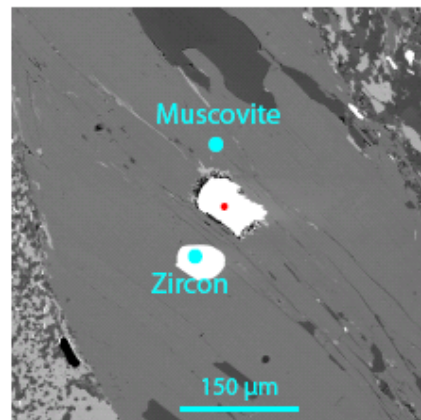


Appendix 11.4. 12: Thin section 09Z-051b. Two monazites have been dated of this sample.

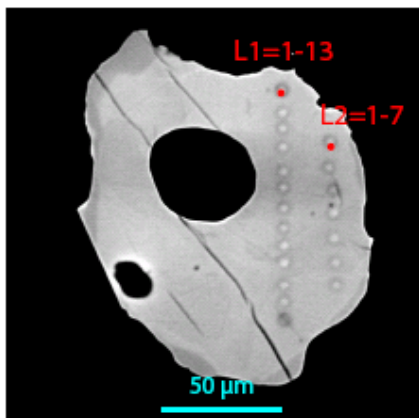
051b-1



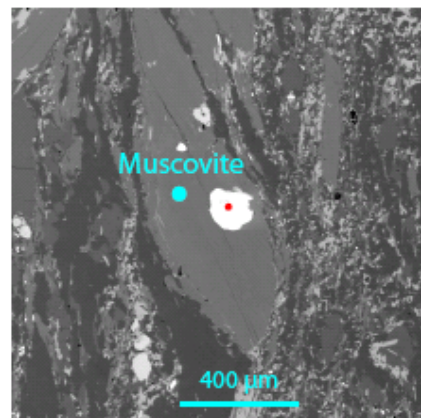
051b-1m



051b-4



051b-4m

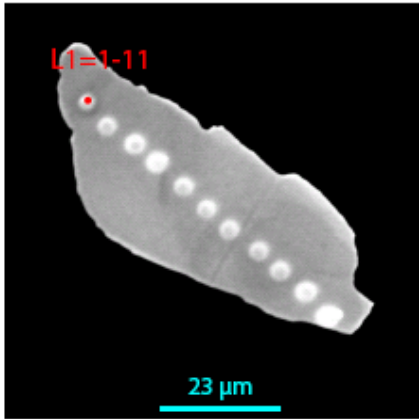


Appendix 11.4. 13: BSE images of dated monazites with their microstructure.

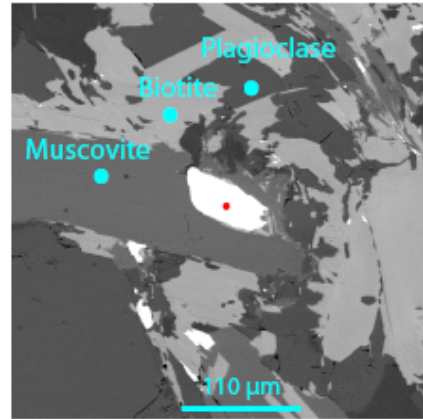


Appendix 11.4. 14: Thin section 09Z-052. Two monazites have been dated of this sample.

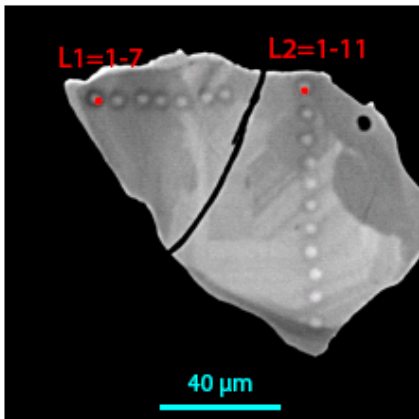
052-1



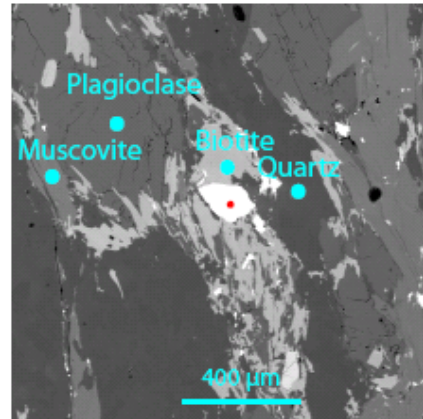
052-1m



052-4



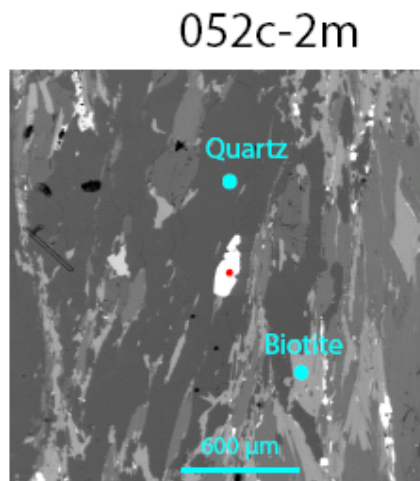
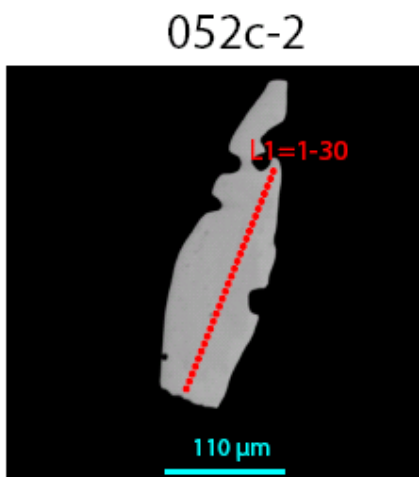
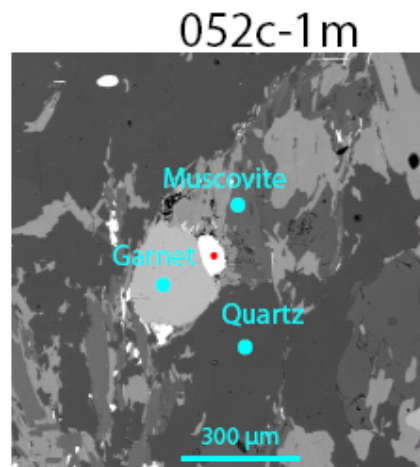
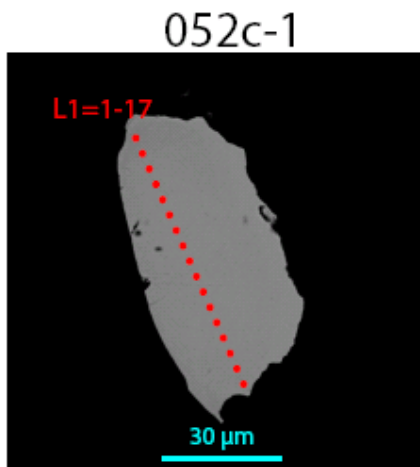
052-4m



Appendix 11.4. 15: BSE images of dated monazites with their microstructure.



Appendix 11.4. 16: Thin section 09Z-052c. Two monazites have been dated of this sample.



Appendix 11.4. 17: BSE images of dated monazites with their microstructure.



Appendix 11.4. 18: Thin section 09Z-052d. No monazites have been dated in this sample.

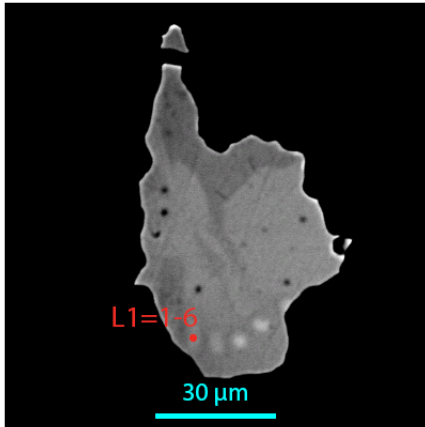


Appendix 11.4. 19: Thin section 09Z-060. No monazites have been dated in this sample.

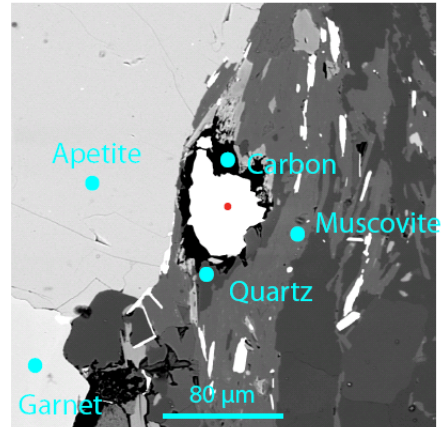


Appendix 11.4. 20: Thin section 09Z-061. One monazite has been dated of this sample.

061-1



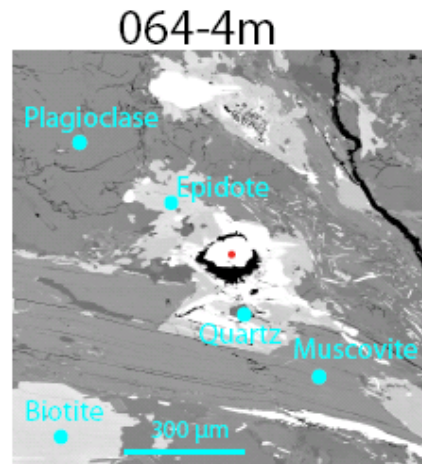
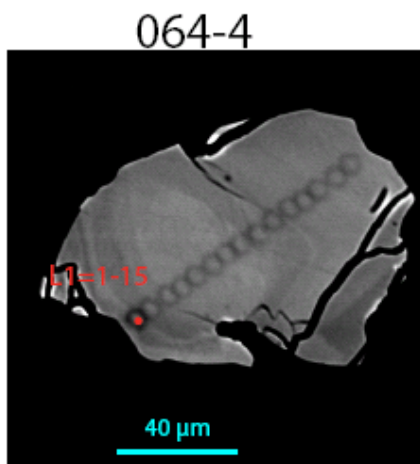
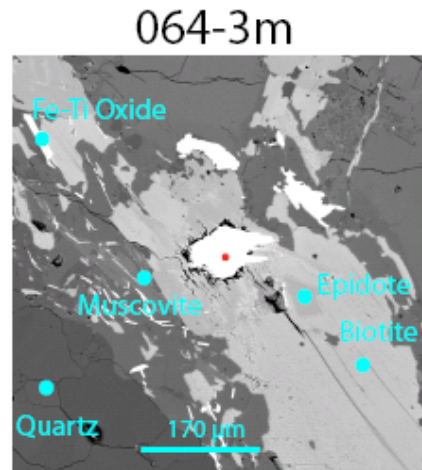
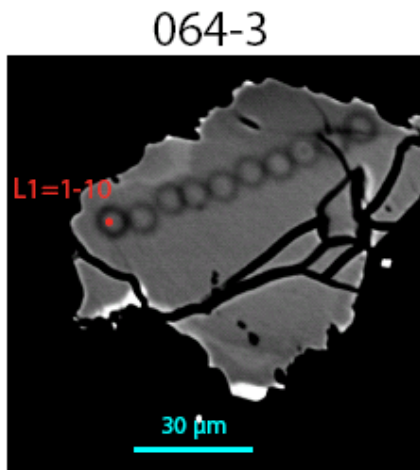
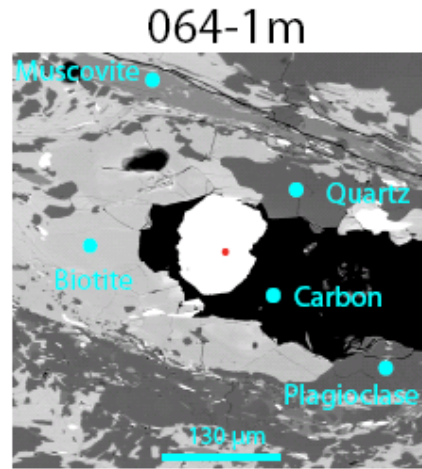
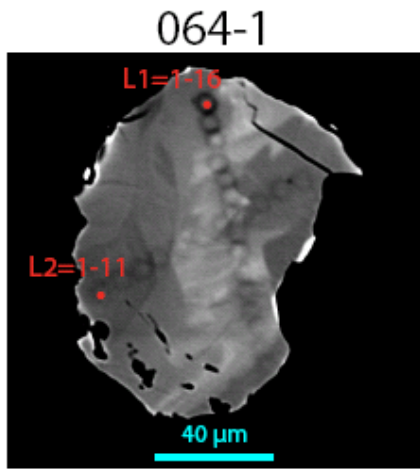
061-1m



Appendix 11.4. 21: BSE image of dated monazite with its microstructure.



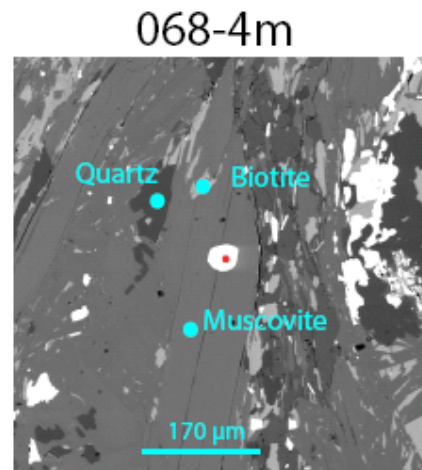
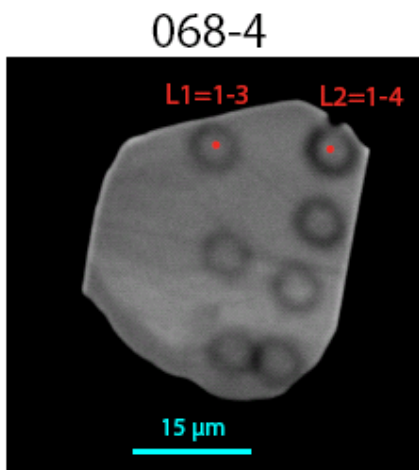
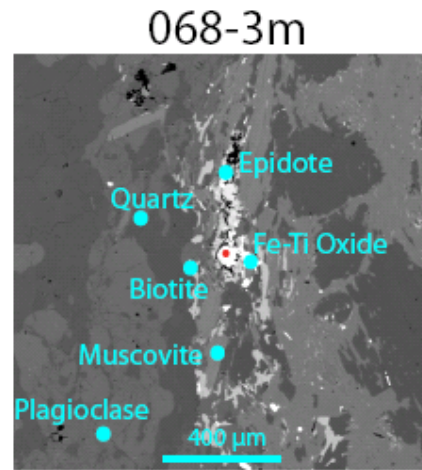
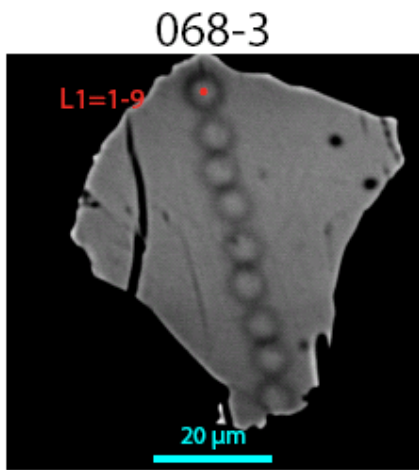
Appendix 11.4. 22: Thin section 09Z-064. Three monazites have been dated of this sample.



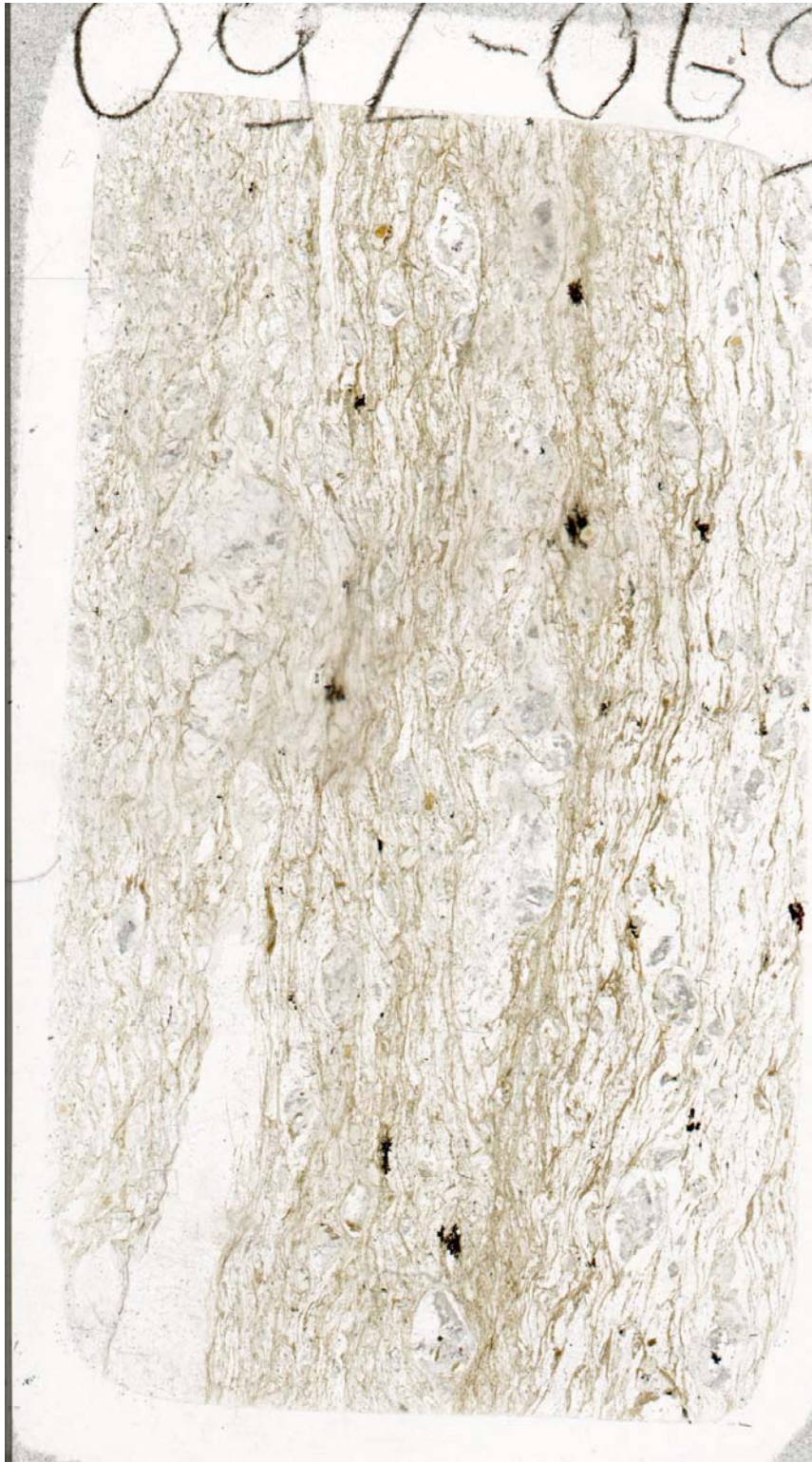
Appendix 11.4. 23: BSE images of dated monazites with their microstructure.



Appendix 11.4. 24: Thin section 09Z-068. Two monazites have been dated of this sample.



Appendix 11.4. 25: BSE images of dated monazites with their microstructure.



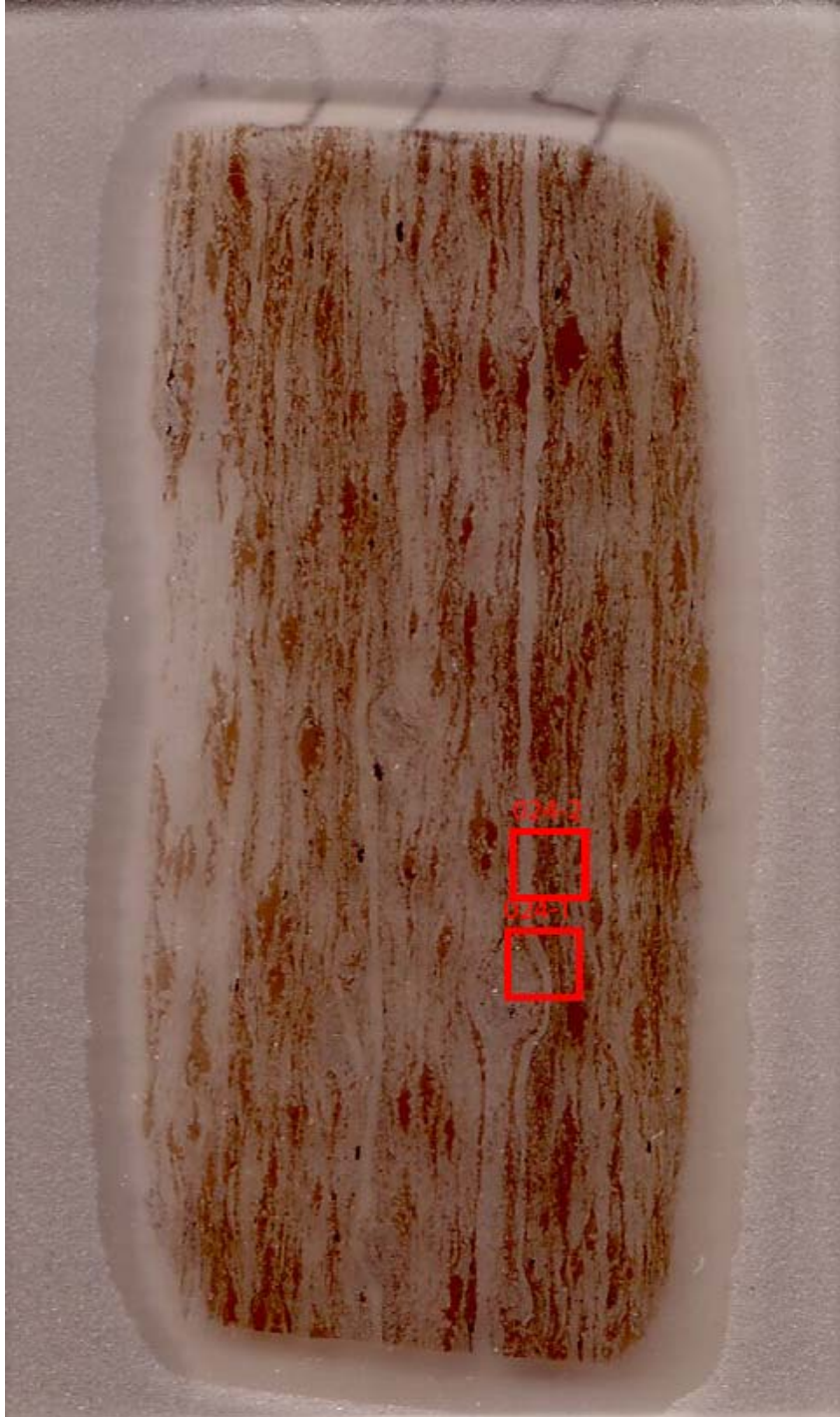
Appendix 11.4. 26: Thin section 09Z-069. No monazites have been dated in this sample.



Appendix 11.4. 27: Thin section 09Z-069II. No monazites have been dated in this sample.

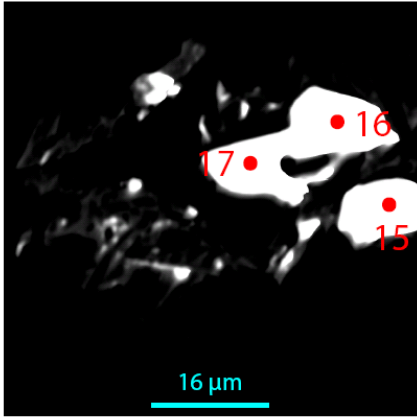
11.5. Thin sections, monazite locations and BSE images Svartsjöbäcken schist.

Samples 024 and 024b belong to the Svartsjöbäcken schist. The numbers of the thin sections corresponds to the locations shown in figure 6 and appendix 11.2.2.

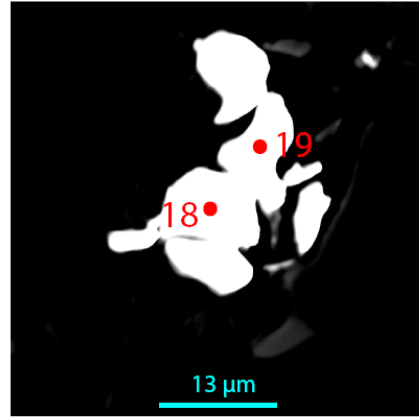


Appendix 11.5. 1: Thin section 09Z-024. Two monazites have been dated of this sample.

024-1



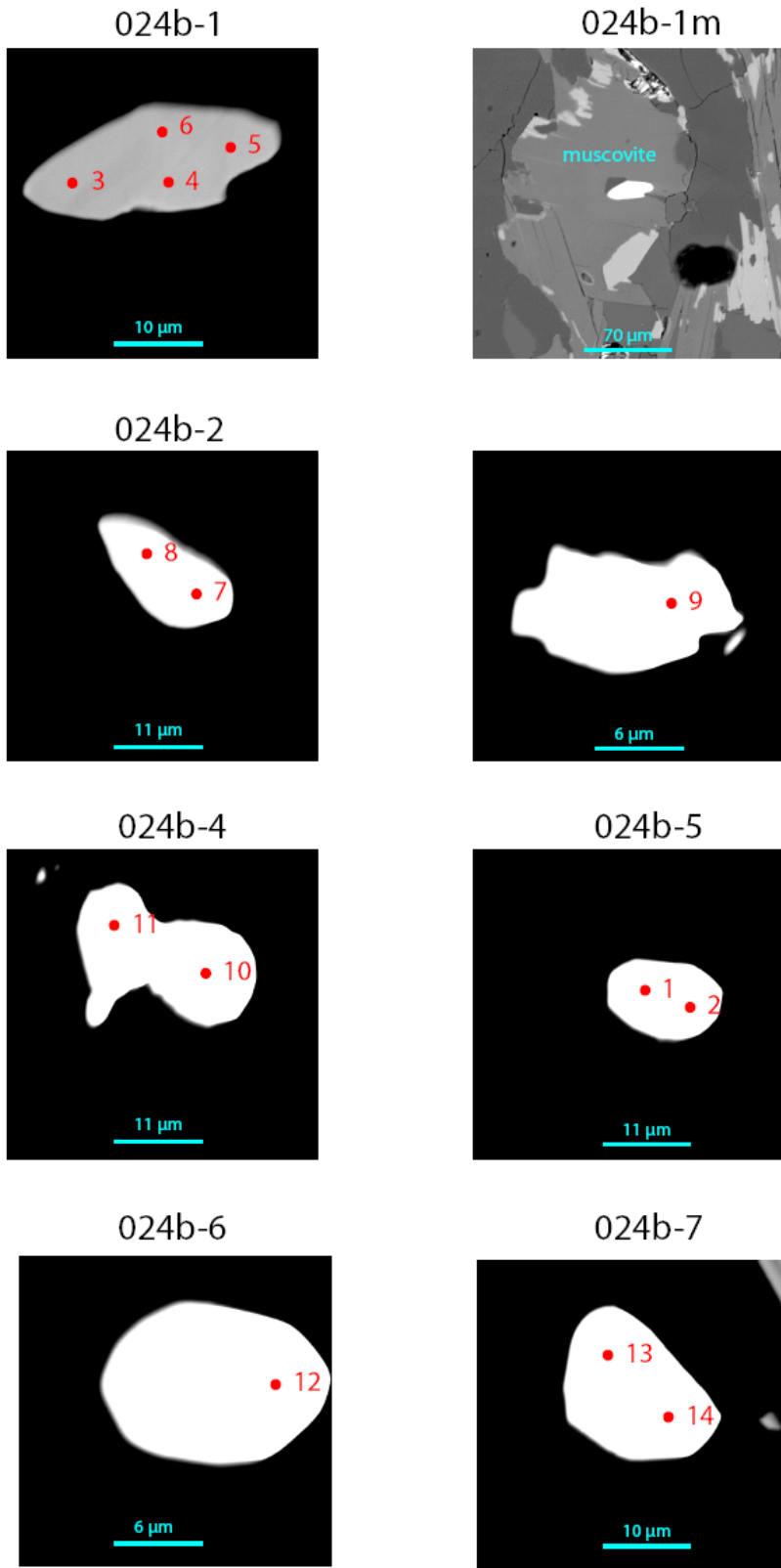
024-2



Appendix 11.5. 2: BSE images of dated monazites.



Appendix 11.5. 3: Thin section 09Z-024b. Seven monazites have been dated of this sample.



Appendix 11.5. 4: BSE images of dated monazites with a microstructure.

11.6. Calculations XRF

FORMULA: General-purpose mineral analysis recalculation (modified after Dave Waters)

Sample 4a Oxygens in formula unit, and weight % of each oxide in the analysis of the XRF

Division by the molecular weight per cation

Multiplication cations props by the number of oxygens associated with each cation in the oxide

Finally, normalise the cation proportions to the correct oxygen total. The factor is (oxygens in formula)/(total oxygen props)

Oxygens in formula 24

	Wt % oxide	Cation props	Oxygen props	Cations p.f.u.	Oxide name	Mol wt per cation	Charge on cation
SiO2	77,41	1,2882	2,5765	10,162	SiO2	60,09	4
TiO2	0,62	0,0078	0,0155	0,061	TiO2	79,9	4
Al2O3	10,54	0,2067	0,3100	1,630	Al2O3	50,97	3
Cr2O3	0,00	0,0000	0,0000	0,000	Cr2O3	76,01	3
Fe2O3	0,00	0,0000	0,0000	0,000	Fe2O3	79,85	3
FeO	2,84	0,0396	0,0396	0,312	FeO	71,85	2
MnO	0,04	0,0005	0,0005	0,004	MnO	70,94	2
MgO	0,88	0,0217	0,0217	0,171	MgO	40,32	2
CaO	0,99	0,0177	0,0177	0,140	CaO	56,08	2
Na2O	1,51	0,0487	0,0243	0,384	Na2O	30,991	1
K2O	3,46	0,0734	0,0367	0,579	K2O	47,1	1
H2O	0,00	0,0000	0,0000	0,000	H2O	9,008	1
Totals	98,28	1,7043	3,0426	13,444			

Appendix 11.6.1: Recalculations of XRF data of sample 4a (after Dave Waters). The red column is the representing the oxygens in the formula unit with their weight % of each oxide in the analysis of the XRF. The yellow column is the result of the red column divided by the mol wt per cation. The green column is a multiplication of cations props by the number of oxygens associated with each cation in the oxide. Finally normalizing the cation proportions to the correct oxygen total has been done in the purple colour. These numbers are used as input for the computer program Theriak-Domino.

FORMULA: General-purpose mineral analysis recalculation (modified after Dave Waters)

Sample 15	Oxygens in formula unit, and weight % of each oxide in the analysis of the XRF			
	Division by the molecular weight per cation			
Oxygens in formula	24	Multiplication cations props by the number of oxygens associated with each cation in the oxide		
		Finally, normalise the cation proportions to the correct oxygen total. The factor is (oxygens in formula)/(total oxygen props)		
	Wt % oxide	Cation props	Oxygen props	Cations p.f.u.
SiO2	73,98	1,2311	2,4621	9,785
TiO2	0,71	0,0089	0,0178	0,071
Al2O3	12,26	0,2405	0,3607	1,911
Cr2O3	0,00	0,0000	0,0000	0,000
Fe2O3	0,00	0,0000	0,0000	0,000
FeO	4,33	0,0603	0,0603	0,479
MnO	0,09	0,0013	0,0013	0,010
MgO	1,40	0,0347	0,0347	0,276
CaO	0,91	0,0162	0,0162	0,129
Na2O	2,10	0,0678	0,0339	0,539
K2O	3,06	0,0650	0,0325	0,516
H2O	0,00	0,0000	0,0000	0,000
Totals	98,83	1,7257	3,0195	13,716

Oxide name	Mol wt per cation	Charge on cation
SiO2	60,09	4
TiO2	79,9	4
Al2O3	50,97	3
Cr2O3	76,01	3
Fe2O3	79,85	3
FeO	71,85	2
MnO	70,94	2
MgO	40,32	2
CaO	56,08	2
Na2O	30,991	1
K2O	47,1	1
H2O	9,008	1

Appendix 11.6.2: recalculations of XRF data of sample 15 (after Dave Waters). The red column is the representing the oxygens in the formula unit with their weight % of each oxide in the analysis of the XRF. The yellow column is the result of the red column divided by the mol wt per cation. The green column is a multiplication of cations props by the number of oxygens associated with each cation in the oxide. Finally normalizing the cation proportions to the correct oxygen total has been done in the purple colour. These numbers are used as input for the computer program Theriak-Domino.

11.7. Mineral list Theriak-Domino

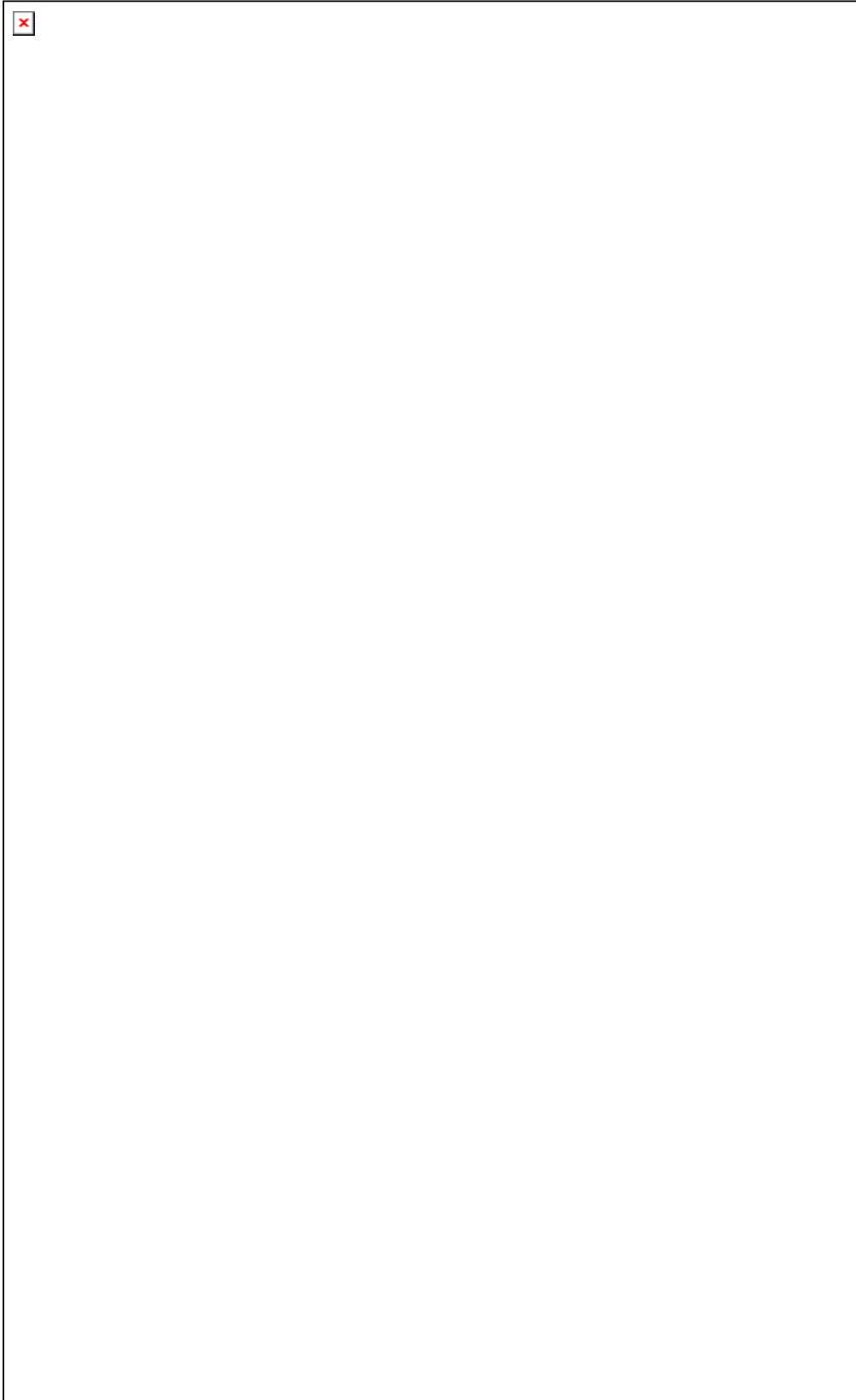
Considered phases	O	Al	Ca	Fe	H	K	Mg	Na	Si	Ti	E
1 "O"	1										
2 "AL"		1									
3 "CA"			1								
4 "FE"				1							
5 "H"					1						
6 "K"						1					
7 "MG"							1				
8 "NA"								1			
9 "SI"									1		
10 "TI"										1	
11 "E"											1
12 AKERMANITE	7		2				1		2		
13 ANTIGORITE	147				62		48		34		
14 BRUCITE	2				2		1				
15 CHRYSOTILE	9				4		3		2		
16 DIASPORE	2	1			1						
17 GEHLENITE	7	2	2						1		
18 HEMATITE	3			2							
19 KALSILITE	4	1				1			1		
20 KAOLINITE	9	2			4				2		
21 LAWSONITE	10	2	1		4				2		
22 ALEUCITE	6	1				1			2		
23 BLEUCITE	6	1				1			2		
24 LIME	1		1								
25 MAGNETITE	4			3							
26 MERWINITE	8		3				1		2		
27 MONTICELLITE	4		1				1		1		
28 NEPHELINE	4	1						1	1		
29 PERICLASE	1						1				
30 PREHNITE	12	2	2		2				3		
31 PYROPHYLLITE	12	2			2				4		
32 RUTILE	2									1	
33 SPHENE	5		1						1	1	
34 TALC	12				2		3		4		
35 WOLLASTONITE	3		1						1		
36 PSEUDOWOLLASTONITE	3		1						1		
37 HEULANDITE	24	2	1		12				7		
38 LAUMONTITE	16	2	1		8				4		
39 STILBITE	25	2	1		14				7		
40 WAIRAKITE	14	2	1		4				4		
41 PUMPELLYITE2	28	5	4		7		1		6		
42 A-QUARTZ	2								1		
43 B-QUARTZ	2								1		
44 COESITE	2								1		
45 CORUNDUM	3	2									
46 ALPHA CRISTOBALITE	2								1		
47 BETA CRISTOBALITE	2								1		
48 LOW TRIDYMITITE	2								1		
49 HIGH TRIDYMITITE	2								1		

50 ANDALUSITE	5	2							1	
51 KYANITE	5	2							1	
52 SILLIMANITE	5	2							1	
53 FAYALITE	4			2					1	
54 FORSTERITE	4						2		1	
55 HERCYNITE	4	2		1						
56 SPINEL	4	2					1			
57 ILMENITE	3			1						
58 GEIKELITE	3						1			
59 GROSSULAR	12	2	3						3	
60 PYROPE	12	2					3		3	
61 ALMANDINE	12	2		3					3	
62 ALBITE	8	1						1	3	
63 K-FELDSPAR	8	1					1		3	
64 ANORTHITE	8	2	1						2	
65 ANNITE	12	1		3	2	1			3	
66 PHLOGOPITE	12	1			2	1	3		3	
67 MARGARITE	12	4	1		2				2	
68 MUSCOVITE	12	3			2	1			3	
69 PARAGONITE	12	3			2			1	3	
70 MCELADONITE	12	1			2	1	1		4	
71 FCELADONITE	12	1		1	2	1			4	
72 FE-STAUROLITE	48	18		4	4				7.5	
73 MG-STAUROLITE	48	18			4		4		7.5	
74 ORTHOENSTATITE	6						2		2	
75 PROTOENSTATITE	3						1		1	
76 FERROSILITE	6			2					2	
77 MG.AL-PYROXENE	6	2					1		1	
78 MG.FE-PYROXENE	6			1			1		2	
79 FE.MG-PYROXENE	6			1			1		2	
80 FE.AL-PYROXENE	6	2		1					1	
81 DIOPSIDE	6		1				1		2	
82 JADEITE	6	1						1	2	
83 HEDENBERGITE	6		1	1					2	
84 CA-AL PYROXENE	6	2	1						1	
85 AMESITE	18	4			8		4		2	
86 PENNINITE	18	1			8		5.5		3.5	
87 FEAMESITE	18	4		4	8				2	
88 FEPENNINITE	18	1		5.5	8				3.5	
89 CORDIERITE	18	4					2		5	
90 HY_CORDIERITE	20	4			4		2		5	
91 FE_CORDIERITE	18	4		2					5	
92 HY_Fe_CORDIERITE	20	4		2	4				5	
93 MG-CHLORITOID	7	2			2		1		1	
94 FE-CHLORITOID	7	2		1	2				1	
95 CLINOZOISITE	13	3	2		1				3	
96 EPIDOTE	13	2	2	1	1				3	
97 ANTHOPHYLLITE	24				2		7		8	
98 TREMOLITE	24		2		2		5		8	
99 FETREMOLITE	24		2	5	2				8	
100 TSCHERMAKITE	24	4	2		2		3		6	
101 PARGASITE	24	3	2		2		4	1	6	

102 FEPARGASITE	24	3	2	4	2			1	6		
103 GLAUCOPHANE	24	2			2		3	2	8		
104 STEAM	1				2						
105 OXYGEN	2										
106 HYDROGEN					2						

Appendix 11.7.1: list of 106 minerals with there accompanying elements. The system only uses input date of the following elements: O, Al, Ca, Fe, H, K, Mg, Na, Si, Ti and E. The minerals highlighted in bright green are applicable within the Marsfjället gneiss.

11.8. Original tectonostratigraphic map Gee (1985)



11.9. Poster

Preliminary Finnmarkian monazite ages in the Central Belt of the Sveve Nappe Complex, N. Jämtland and S. Västerbotten, Sweden

M. Gademan, M.A. Hogerwerf and H.L.M. van Roermund
Structural Geology Group, Institute of Earth Sciences, Utrecht University, Budapestlaan 4, 3506 TA, Utrecht, The Netherlands.



Introduction

The Scandinavian Caledonides consists of a series of Nappe Complexes that were transported, in early Paleozoic times, from west to east over the Baltic Shield (inset fig 1). The investigated metamorphic complex studied here, called the Sveve Nappe Complex (SNC) in Sweden, defines the lower part of the Upper Allochthon in the counties of N. Jämtland and S. Västerbotten (fig 1). Here the SNC is subdivided into three NS running belts called, from top to bottom, the Western, Central and Eastern Belts (Zwart, 1974). The Western Belt is overlain by the KMI Nappe Complex (KNC), the Eastern Belt is overlain by nappes of the lower Allochthon.

The metamorphic grade (=temp. °C) of the SNC increases from the structural top (Western Belt: lower amphibolite facies) downwards (Central Belt: upper amphibolite- to granulite facies) and then decreases again (Eastern Belt: lower amphibolite- to upper greenschist facies). In addition the Central Belt encompasses three different metamorphic facies: northern part, HP granulite facies (Thouw, 1969); central part, eclogite facies (Van Roermund, 1985) and southern part, LP granulite facies (Van der Sijp, 1976). Only the eclogite facies mineral assemblage in the Central Belt is dated as being 450 Ma (Bruetner & Van Roermund, 2008). This change in metamorphic facies, restricted exclusively to the Central Belt of the SNC, has never been explained and forms the topic of our research project.

Method

The Electron Micro Probe (EMP) age dating technique, developed by Suzuki and Adachi (1991), was used to date monazite.

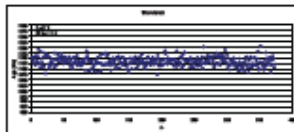


Fig 2. Simultaneous EMP age-results of measurements on a monazite standard with known age (1125 Ma).

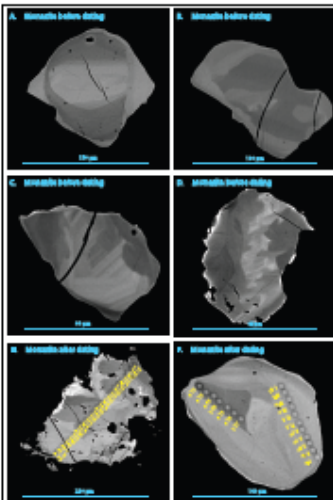


Fig 3. A-F Back-scattered electron images of representative monazite microstructures. In E and F spots with corresponding age (in yellow) are also given.

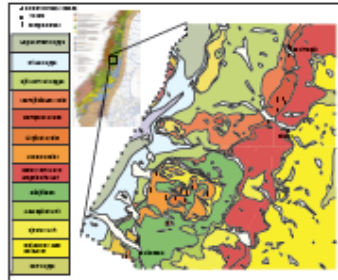


Fig 1. Geological map of the fieldwork area (modified after bedrock maps of the SGU). Inset (top left): Tectonic map of the Scandinavian Caledonides (taken from IGCP project No. 27).

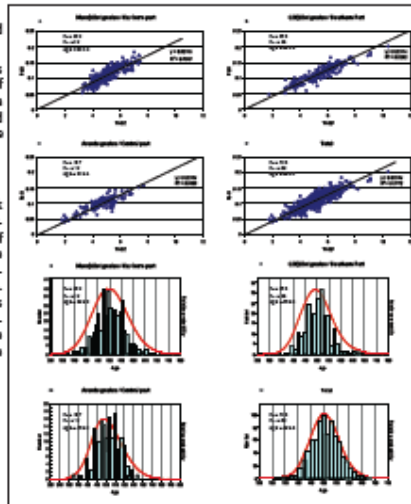


Fig 4. A-D: ThO_2 vs PbO isochron plots with corresponding isochron ages. E-H: age vs number histograms with corresponding probability curves and peak ages. n_1 is number of analysts n_2 is number of measured monazites

Preliminary conclusions

- ThO_2 and PbO data are consistent with a single monazite growth event
- Monazite formed at ~500 Ma (Finnmarkian)

Appendix 11.9. 1: Illustration of the poster that was presented on the Nordic Geological Winter meeting, Oslo.

11.10. Overview digital MSc Thesis M.A.Hogerwerf

Name	Directory	Word/PDF/Excel	Tabs Excel
Overview digital MSc Thesis M.A.Hogerwerf	Appendices	Appendices.doc	
		Appendices.pdf	
	Avardo & Sjouten	HP.xls	HP
		HPmodified.xls	Locations EMP
	EMP mineral analyses	EMP.xls	Garnet K-Feldspar Plagioclase Biotite White Mica
	Marsfjallen	Marsfjallen.xls	Marsfjallen
		Marsfjallen modified.xls	Locations EMP
		Backscatter coefficient.xls	
	Standard	Standard locations.doc	
		Standard modified.xls	
		Standard.xls	
	Svartsjobacken	Svartsjobacken.xls	Svartsjobacken
			Locations EMP
Thesis	MSc Thesis M.A.Hogerwerf.doc		
	MSc Thesis M.A.Hogerwerf.pdf		
XRF	Raw XRF data.xls		